![Universiteit Leiden - The Netherlands]

An integrated metabolomics-based model, and identification of potential biomarkers, of perfluorooctane sulfonic acid toxicity in zebrafish embryos

Annunziato, M.; Bashirova, N.; Eeza, M.N.H.; Lawson, A.; Fernandez-Lima, F.; Tose, L.V.; ... ; Berry, J.P.

Environmental Toxicology

An Integrated Metabolomics-Based Model, and Identification of Potential Biomarkers, of Perfluorooctane Sulfonic Acid Toxicity in Zebrafish Embryos

Mark Annunziato,[a,b,c] Narmin Bashirova,[d] Muhamed N.H. Eeza,[e] Ariel Lawson,[b] Francisco Fernandez-Lima,[a,b,c] Lilian V. Tose,[a,b,c] Jörg Matysik,[d] A. Alia,[e,f] and John P. Berry[a,b,c],*

[a]Institute of Environment, Florida International University, Miami, Florida, USA
[b]Department of Chemistry and Biochemistry, Florida International University, Miami, Florida, USA
[c]Biomolecular Science Institute, Florida International University, Miami, Florida, USA
[d]Institute for Analytical Chemistry, University of Leipzig, Leipzig, Germany
[e]Institute for Medical Physics and Biophysics, University of Leipzig, Leipzig, Germany
[f]Leiden Institute of Chemistry, Leiden University, Leiden, The Netherlands

Abstract: Known for their high stability and surfactant properties, per- and polyfluoroalkyl substances (PFAS) have been widely used in a range of manufactured products. Despite being largely phased out due to concerns regarding their persistence, bioaccumulation, and toxicity, legacy PFAS such as perfluorooctanesulfonic acid (PFOS) and perfluorooctanoic acid continue to persist at high levels in the environment, posing risks to aquatic organisms. We used high-resolution magic angle spinning nuclear magnetic resonance spectroscopy in intact zebrafish (*Danio rerio*) embryos to investigate the metabolic pathways altered by PFOS both before and after hatching (i.e., 24 and 72 h post fertilization [hpf], respectively). Assessment of embryotoxicity found embryo lethality in the parts-per-million range with no significant difference in mortality between the 24- and 72-hpf exposure groups. Metabolic profiling revealed mostly consistent changes between the two exposure groups, with altered metabolites generally associated with oxidative stress, lipid metabolism, energy production, and mitochondrial function, as well as specific targeting of the liver and central nervous system as key systems. These metabolic changes were further supported by analyses of tissue-specific production of reactive oxygen species, as well as nontargeted mass spectrometric lipid profiling. Our findings suggest that PFOS-induced metabolic changes in zebrafish embryos may be mediated through previously described interactions with regulatory and transcription factors leading to disruption of mitochondrial function and energy metabolism. The present study proposes a systems-level model of PFOS toxicity in early life stages of zebrafish, and also identifies potential biomarkers of effect and exposure for improved environmental biomonitoring. *Environ Toxicol Chem* 2024;00:1–19. © 2024 SETAC

Keywords: Aquatic toxicology; Contaminants; Perfluoroalkyl substance; Perfluorooctane sulfonate; Toxicity mechanisms

INTRODUCTION

Per- and polyfluoroalkyl substances (PFAS) are a group of fluorinated compounds that have been used for an array of industrial applications since the 1950s. The unique stability of PFAS, due to the high electronegativity of fluorine, as well as their surfactant properties, have led to their incorporation into numerous manufactured products such as fabric protectors, food packaging, and fire-fighting foams. Because PFAS compounds are chemically stable, concerns about their environmental persistence, as well as their bioaccumulation and toxic potential, have led to some of the so-called legacy PFAS including perfluorooctanesulfonic acid (PFOS), and its carboxylic acid analog, perfluorooctanoic acid (PFOA), being largely phased out (Wang et al., 2009). However, owing to their decades of use, and inherently high stability, these legacy PFAS persist at some of the highest levels in the environment.

Of the legacy PFAS, PFOS remains one of the most frequently detected in the environment, particularly in aquatic systems, and is found at some of the highest concentrations in marine and freshwater biota, including vertebrate species such as fish, which represent key ecological receptors of these pollutants (Lee et al., 2020; Valsecchi et al., 2021). When detected,

PFOS is typically found at concentrations in surface water <0.1 µg L^{-1} (i.e., parts-per-billion [ppb]), and most often in the parts-per-trillion (ppt) range, although concentrations of up to 0.6 ppb have been detected in rivers downstream of fluorochemical manufacturing facilities. Despite typically low concentrations found in the aquatic environment, however, PFOS has been shown to bioaccumulate in fish, with reported concentrations over 8000-fold higher than in surface water (Sinclair et al., 2006). For example, PFOS was detected at 7760 ppb wet weight in the liver of plaice (*Pleuronectes platessa*; Hoff et al., 2003), and at 9031 ppb wet weight for wild Gibel carp (*Carassius auratus gibelio*) in Belgium (Hoff et al., 2005). In addition to adult fish, PFOS has been detected in fish eggs (145–381 ppb) from lake whitefish (*Coregonus clupeaformis*) in the United States (Kannan et al., 2005), as well as eggs from adult fish exposed in laboratory settings, specifically suggesting that PFOS can be parentally transferred to offspring (Ankley et al., 2005).

Alongside studies of apparent bioaccumulation, numerous toxicological studies utilizing fish have also connected PFOS exposure to toxicity and an array of adverse effects including altered reproductive function, developmental deformities, endocrine disruption, and hepatotoxicity (Hagenaars et al., 2008; Kang et al., 2019; Shi et al., 2008, 2009). With relevance to aquatic biota, a number of studies have investigated the toxicity of PFOS (and many other PFAS) in the zebrafish (*Danio rerio*), as an established laboratory model, and more specifically, early life (i.e., embryonic, larval) stages of this species (Huang et al., 2010; Krupa et al., 2022; Mylroie et al., 2021; Shi et al., 2008). These studies have indeed identified a range of potential toxicological endpoints, and notably, the zebrafish embryo model in particular has enabled studies that elucidate the role of developmental stage, and associated stage-dependent mechanisms and targets. With respect to the latter issue, a recent study (Vogs et al., 2019) has specifically pointed, for example, to a possible role of the protective chorion of zebrafish embryos with regard to the toxicity of PFOS, and suggested a biphasic two-compartment toxicokinetic model whereby the chorion represents a significant barrier to PFOS prior to embryo hatching. The mechanism(s) of how these toxic effects are connected, however, remains unclear in part due to the limited scope of studies that typically focus on only one, or small subset of, specific biological target(s).

To gain a more detailed understanding of toxicity, and associated adverse health impacts, *systems-level* approaches (particularly omics,e.g., transcriptomics, proteomics, metabolomics) have most recently been employed to enable a more holistic interpretation of biochemical perturbations caused by exposure to PFAS including PFOS (Dorts et al., 2011; Lee et al., 2021; Martínez et al., 2019; Ortiz-Villanueva et al., 2018). Among these omics approaches, the targeted and nontargeted analysis of metabolic perturbations, or *metabolomics*, has shown considerable promise, through the use of sophisticated analytical platforms such as high-resolution mass spectrometry (e.g., Orbitrap, quadrupole time-of-flight [QToF]), typically coupled to analytical separation by, in particular, liquid chromatography (i.e., LC–mass spectrometry [MS]) and nuclear magnetic resonance (NMR) spectroscopy including, in particular, magic angle spinning (MAS) NMR. Because metabolites are the downstream products of transcription and translation, as well as post-translational modifications, metabolomics can provide a direct view of the current cellular state of the system after toxic exposure. These analytical techniques when combined with animal models including fish species such as the zebrafish, which is a well-established laboratory model, have emerged as a powerful approach to study the toxicological pathways of a wide range of environmental toxicants including PFAS (Gebreab et al., 2020; Ortiz-Villanueva et al., 2018).

To assess the toxicological effects of PFOS, and subsequently its environmental health and ecotoxicological impacts, the present study specifically utilized *high-resolution magic angle spin* (HRMAS) NMR-based metabolic profiling, alongside *nontargeted* LC-MS analysis of lipids, of *intact* zebrafish embryos to allow a holistic picture of the biological pathways affected by PFOS exposure during this critical and sensitive developmental stage of teleost fish as both relevant ecological receptors, and potential models of vertebrate toxicity. Numerous previous studies utilizing HRMAS NMR coupled to the zebrafish embryo model have, in fact, shown that this approach is capable of highly reproducible quantitation of the concentrations of a range of major metabolites, which, in turn, has enabled development of integrated models for a wide range of environmental toxicants (Annunziato et al., 2022, 2023; Bashirova et al., 2023; Berry et al., 2016; Eeza et al., 2022; Gebreab et al., 2020; Roy et al., 2017; Zuberi et al., 2019). Whereas HRMAS NMR allows reproducible quantitation of *major* metabolites, it does not, however, provide access to the full breadth of potentially relevant metabolites; a more comprehensive analysis of metabolites is, on the other hand, potentially accessible by techniques such as LC–MS. One example, in this regard, is the application of LC–MS-based methods for profiling both specific lipids and/or lipid classes (i.e., lipidomics). In one relevant, previous lipidomics study, for example, glycerophospholipids were specifically found to be altered, and in turn, linked to alterations in absorption of the yolk sack, in PFOS-exposed zebrafish embryos (Ortiz-Villanueva et al., 2018). Alongside HRMAS NMR, therefore, metabolite profiling was supplemented in the present study with high-resolution MS, specifically, state-of-the-art trapped ion mobility (TIMS) QToF tandem MS (MS/MS)-based lipidomics. Together this approach enabled the identification and characterization of a wide range of relevant cellular and metabolic pathways altered by PFOS exposure, and accordingly, an integrated systems-level model of PFOS toxicity is proposed.

METHODS

Chemicals and reagents

Perfluorooctane sulfonic acid, as the potassium salt (≥98% purity; CAS 2795-39-3), and all other chemicals (i.e., deuterated phosphate buffer and reference standard for NMR), were purchased from Sigma-Aldrich, unless otherwise specified. Working solutions of PFOS for exposure of zebrafish, as part of the toxicological and metabolomics assessments, were prepared by

dissolution in dimethyl sulfoxide (DMSO), and subsequent dilution into embryo medium (Brand et al., 2002) with a final concentration of DMSO, in all cases, <0.001%. Furthermore, although previous studies have suggested that some PFAS can be unstable in DMSO, degradation was only observed over several hours to days (Zhang et al., 2021), so we only used DMSO briefly to facilitate dissolution, and did not store the PFOS in the solvent for more than 1 h, and typically for 30 min or less.

Fish rearing and breeding

To assess PFOS toxicity, embryos of zebrafish (*Danio rerio*) from the PSA line were acquired from the University of Miami Rosenstiel School of Marine and Atmospheric Science. The zebrafish were reared and bred using established methods (Gebreab et al., 2020; Weiss-Errico et al., 2017). The collected eggs were washed with system water and placed in Petri dishes with approximately 30 mL of E3 medium (Brand et al., 2002) and approximately 120 eggs/plate. Prior to 24- or 72-h post fertilization (hpf) exposures, embryos were kept in an incubator (14:10-h light:dark, 28 °C) and examined daily to remove any dead or moribund embryos. For 24-hpf exposures, embryos were transferred to test plates just prior to exposure. For 72-hpf exposures, *unhatched* embryos were transferred to wells of test plates 24 h prior to this exposure time (at ~48 hpf); embryos do not hatch, under the rearing conditions used, until 72 hpf, and transfer of unhatched 48-hpf embryos was done both to facilitate transfer by pipet, and to eliminate any potential damage that might occur during the when transfer of hatched and free-swimming embryos. Rearing and breeding was conducted based on protocols approved by the University of Miami's Institutional Animal Care and Use Committee (20-006 LF), and performed by trained personnel.

To conduct NMR metabolomic studies, embryos of zebrafish (OBI/WIK line) were procured from the UFZ Helmholtz Centre for Environmental Research. Adult zebrafish were raised in recirculating aquarium systems using established techniques (van Amerongen et al., 2014). Breeding involved placing three adult males and four females in breeding tanks with mesh egg traps (Ehret) the night before collection. The next morning, approximately 120 embryos were added to each Petri dish containing 40 mL of fresh embryo medium (International Organization for Standardization [ISO], 2007), and kept in an incubator with a light cycle of 14:10-h light:dark at 28 °C. Dead or malformed embryos were removed daily before fresh embryo medium was added. All experimental procedures adhered to German animal protection standards and were approved by the Government of Saxony, Landesdirektion Leipzig, Germany (Aktenzeichen 75-9185.64).

Assessment of embryotoxicity of PFOS

To determine acute toxicity and establish exposure concentrations for HRMAS NMR experiments, the lethality to zebrafish embryos (PSA line) was evaluated across a range of PFOS concentrations, and over two different exposure time periods (to assess, in part, differences in sensitivity not only at different stages of development, but also at different exposure durations). Exposures and toxicity assessments utilized previously established protocols (Berry et al., 2007; Gebreab et al., 2020; Weiss-Errico et al., 2017). Prior to the assays, a range of effective exposure concentrations (i.e., 10, 25, 50, 75, 100, 125, 150, and 175 ppm PFOS) was established in preliminary studies, and exposures were performed in triplicate ($n = 3$) using polypropylene 24-well plates (Evergreen Scientific), with each well containing five embryos ($n = 5$) in 1.5 mL of E3 medium. Exposure times of 24 and 72 hpf were chosen to specifically correspond, respectively, to developmental stages at which either the chorion is present (i.e., unhatched at 24 hpf), or embryos have fully hatched and the chorion is not present (i.e., 72 hpf). In both cases, embryotoxicity was assessed at 96 hpf, following either 72 or 24 h of static exposure to PFOS (without replenishment) for 24- and 72-hpf exposures times, respectively. Embryo lethality was assessed by observing cessation of movement, and the absence/presence of a heartbeat, using a dissecting light microscope. Median lethal concentrations (LC50s) were calculated using Probit analysis in SPSS (Ver. 26.0; IBM). All toxicity assays were conducted at Florida International University (FIU), under protocols approved by the FIU Animal Care and Use Committee (IACUC-19-085-AM01).

Visualization of ROS in zebrafish embryos

The generation of reactive oxygen species (ROS) to assess the role of oxidative stress in PFOS toxicity was observed in intact zebrafish embryos through the fluorescence of intracellularly oxidized 2′,7′-dichlorofluorescein. This was done following exposure of 72-hpf zebrafish embryos (OBI/WIK line) to 10 ppm PFOS for 24 h, alongside untreated controls of embryo medium with or without added DMSO, as previously described (Annunziato et al., 2022). At 96 hpf, embryos were treated with 1 mM of the nonfluorescent cell-permeative probe chloromethyl-2′,7′-dihydrodichlorofluorescein diacetate (CM-H2DCFA; Invitrogen no. LSC6827), dissolved in 4% DMSO, to a final concentration of 10 µM. Incubation was done for a total of 60 min, and excess CM-H2DCFA in the medium was removed through three washes. Embryos were then placed on a borosilicate glass coverslip slide in a solution containing the anesthetic ethyl 3-aminobenzoate methanesulfonate (1 mg mL^{-1}). After a 3-min delay for immobilization, images were taken using an inverted laser-scanning confocal microscope (Leica DMi8/TL LED; Leica Microsystems), with an excitation wavelength of 485 nm and emission wavelength of 530 nm. A Leica HC PL Apo CS2 (5×/0.15 Dry) objective and the Leica Application Suite X (LAS X) software package, Ver. 3.1.5, were used for image acquisition.

Exposure of embryo and sample preparation for HRMAS NMR

Previously established protocols (Annunziato et al., 2022) were used to expose approximately 120 zebrafish embryos (OBI/WIK line) to 10 ppm PFOS in replicates ($n = 6$) at both 72

and 24 hpf—alongside negative controls of embryos at the same developmental stages exposed to 0.001% DMSO only—for subsequent HRMAS NMR analysis. Static exposures (with replenishment of PFOS) were conducted in 100-mm polystyrene Petri dishes containing 25 mL of embryo medium (ISO, 2007) for either 72 h (24–96 hpf), or 24 h (72–96 hpf). During exposure, all dead or moribund embryos were removed to avoid any effects of mortality or moribundity on observed metabolic profiles; in accordance with prior assessment of toxicity, mortality at the 10-ppm exposure concentrations was <2% for both exposure times. After exposures (at 96 hpf), excess PFOS and media were removed by washing the embryos with Milli-Q water, and 100 embryos were collected, snap-frozen, and stored at −80 °C until analysis. The exposures were conducted in accordance with German animal protection standards approved by the Government of Saxony (Aktenzeichen 75-9185.64), and guidelines of the European Union, Directive 2010/63/EU, which permit the use of embryonic and early larval stages of fish. Prior to NMR analysis, 100 embryos were transferred to a 4-mm zirconium oxide rotor (Bruker BioSpin). To serve as a chemical shift reference, 10 µL of deuterated phosphate buffer (100 mM, pH 7.0) containing 0.1% (w/v) 3-trimethylsilyl-2,2,3,3-tetradeuteropropionic acid (TSP) was added.

HRMAS NMR and data analysis

All NMR experiments were performed using a Bruker DMX 600-MHz NMR magnet with a proton resonance frequency of 600 MHz, and a 4-mm HRMAS dual $^1H/^{13}C$ inverse probe with a magic angle gradient, and spinning rate of 6 kHz. The experiments were carried out at a temperature of 277 K using a Bruker BVT3000 control unit, and the acquisition and processing of data were performed in Bruker TOPSPIN Ver. 4.0.6 software. A zgpr pulse sequence with water suppression was applied for one-dimensional ^1H HRMAS NMR spectra. Each one-dimensional spectrum was obtained using a spectral width of approximately 12,000 Hz, domain data points of 4 k, a number of averages of 128 with zero dummy scans, an acquisition time of 170 ms, and relaxation delay of 2 s. The spectra were processed by an exponential window function with a line broadening of 1 Hz, and zero-filled before Fourier transformation.

The resulting NMR spectra were manually phased and automatically baseline-corrected using TOPSPIN, and metabolites were quantified using Chenomx NMR Suite 8.2. The 600-MHz library from Chenomx was utilized, which uses the concentration of a known reference signal (in this case, TSP) to determine the concentration of individual compounds. The concentrations of metabolites were subsequently normalized to total creatine (tCr), that is, creatine and creatine phosphate. Statistical analysis of NMR quantification was done using Metaboanalyst, with differences in individual metabolites evaluated using a t test with a p value < 0.05 considered significant. Two-dimensional principal component analysis scores plots with visualized 95% confidence regions were constructed using Metaboanalyst software.

LC–MS lipidomics

To perform lipidomic analyses, approximately 100 zebrafish embryos (PSA line at 72 hpf) were exposed for 24 h to 10 ppm PFOS, as described for HRMAS NMR analyses. To extract lipids, 100 embryos were homogenized in 1 mL of a mixture of methanol and water (1:1, v/v) along with 10 µL of labeled internal standard (EquiSplash Lipidomix; Avanti Polar Lipids). A subsequent addition of chloroform (1 mL) was made to the sample, which was then sonicated for 15 min; the sample was then centrifuged at 4500 rpm for 20 min, and the chloroform layer was collected, and dried under nitrogen gas. The sample was then reconstituted with a 50/50 acetonitrile/water mixture prior to analysis.

Chromatographic separation was performed using an LC-20 CE ultrafast liquid chromatograph (Shimadzu) with a Accucore C30 column (Thermo Fisher Scientific). The mobile phase consisted of solvent A (30% acetonitrile [ACN]; 40% water; 30% isopropyl alcohol [IPA]) and solvent B (10% ACN; 5% water; 85% IPA) under the following conditions: sample injection at 0% B and hold for 1 min; from 1 to 5.6 min increase to 55% B, and hold until 6.4 min; increase to 65% B at 6.4 min, and hold until 24 min; increase to 88% B at 24 min, and hold until 40.8 min; increase to 95% B until 48.1 min; after 48.1 min, decrease to 35% B, and hold until 56 min; decrease to 0% B at 56 min, and hold until 60 min. The mobile phase flow rate was 200 µL min^{-1} with an injection volume of 5 µl.

To obtain lipid profiles, TIMS-q-TOF MS/MS analysis was performed using a timsTOF PRO 2 instrument (Bruker Daltonics) with an Apollo II ESI Source design (Bruker Daltonics) in positive ion mode. The ionization source parameters consisted of a 4500-V capillary voltage, 800-V end plate offset, 4.0-bar nebulizer pressure, 4.0-L/min dry gas, and 250 °C dry heater. A tuning mix calibration standard from Agilent Technologies was used for mobility and m/z internal calibration for all spectra. Between each LC run, a blank and a verification standard were analyzed for quality control purposes. To account for blank peaks, LC peak area subtraction was utilized. Fatty acid assignment, based on MS/MS, was carried out using TIMS-q-TOF MS/MS, which allowed for parallel accumulation serial fragmentation. Bruker Compass MetaboScape Ver. 8.0.1, and the spectral library from MetaboBASE (Bruker Daltonics), were used to identify more than 200 lipids. Lipid concentrations were normalized using deuterated (i.e., ^2H-labeled) internal standards of 13 lipids (EquiSplash Lipidomix; Avanti Polar Lipids) to adjust for variations in extraction efficiency. Individual annotated lipids were specifically quantified by normalization to the deuterated standard, diglyceride (DG) 15:0/18:1-d7, and compared by Student's t test ($p < 0.05$) to identify any statistical significance between PFOS-treated and control embryos. Any lipids that were not consistently detected in all samples were excluded from the statistical analysis.

RESULTS AND DISCUSSION

Embryotoxicity of PFOS

To determine appropriate exposure concentrations and times for subsequent NMR-based metabolomics (and other studies, e.g., ROS visualization, lipidomics), the embryotoxicity of PFOS was assessed in zebrafish embryos at two different exposure periods, that is, 24 to 96 and 72 to 96 hpf. Dose-dependent toxicity of PFOS was observed for both exposure times over a nominal concentration range of 10 to 100 ppm (Figure 1) with LC50 values of 48 ppm (95% CI = 41–55 ppm) and 64 ppm (95% CI = 54–74), respectively, being comparable to those previously reported for PFOS in the zebrafish embryo model (Hagenaars et al., 2011). Notably, lethal concentrations of PFOS in the present, and past, studies are substantially, and as much as 10-fold, higher than its carboxylic acid analog, PFOA (see Pecquet et al., 2020). It has been previously suggested that this is likely due, in large part, to a considerably (as much as 100-fold) higher uptake (e.g., the bioconcentration factor) of PFOS, compared with PFOA, in the zebrafish embryo (Warner et al., 2022).

Although, lower toxic concentrations (i.e., LC50s in the lower ppm range) for PFOS-exposed zebrafish embryos have been previously reported (Huang et al., 2010; Mylroie et al., 2021; Shi et al., 2008), these have been consistently observed only at later (>120 hpf) developmental stages. In addition, interestingly, one very recent study has even reported sub-ppm LC50 values, specifically following embryo exposure, in subsequent larval/juvenile stages after 30 days post exposure (Krupa et al., 2022). These findings support the role of the developmental stage in the toxicity of PFOS in the zebrafish model. In the present study, however, the corresponding LC50 values were not significantly different for 96-hpf zebrafish exposed at 24 and 72 hpf. This finding is surprising, because previous studies in the zebrafish embryo (Huang et al., 2010) have reported a steady uptake of PFOS from the exposure medium, over 24 to 120 hpf, with a more than 10-fold increase in embryo concentration. Aligned with our present observation, a recent study of PFOS in the zebrafish embryo model likewise did not find significant lethality at
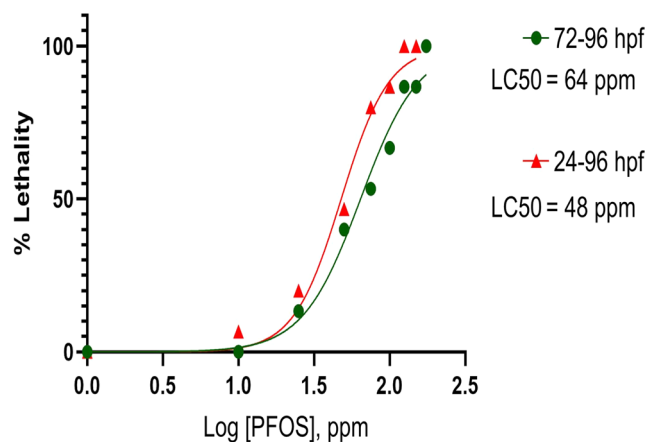
lower, that is, ppm, concentrations until 96 hpf (Mylroie et al., 2021). This latter study, furthermore, investigated the possible role of the protective chorion: survivorship, however, was not found to be *significantly* different for chorionated and dechorionated embryos (even at 120 hpf), suggesting that hatching, that is, loss of chorion (which occurs at ~72–120 hpf) is not a significant contributor to the onset of toxicity at these developmental stages. Taken together, it is suggested that PFOS toxicity at ≥96 hpf is rather associated with the development of relevant biochemical, molecular, or cellular targets.

Based on these results, a nominal exposure concentration of 10 ppm was chosen for subsequent experiments (for both exposure times) to assess the effects of PFOS on metabolic profiles with the aim of elucidating impacts on biochemical, molecular, and cellular pathways. An exposure concentration well below the calculated LC50 was chosen, to avoid any nonspecific effects on metabolite profiles caused by embryo mortality and morbidity, while ensuring a measurable metabolic response. Indeed, <2% mortality or morbidity was observed for embryos exposed to this concentration in both toxicity assessments, and subsequent exposures for NMR and visualization studies, with a percentage mortality similar to that of control embryos specifically exposed to <0.001% DMSO—used as a solvent vehicle—in the embryo medium.

Visualization and localization of ROS in PFOS-exposed embryos

Visualization of ROS production (by fluorescence) enabled the localization of tissue-specific oxidative stress in intact zebrafish embryos (Figure 2). Apparent ROS production was observed in negative controls including both untreated and 0.001% DMSO only (i.e., vehicle) treated embryos within the gastrointestinal (GI) tract including the stomach and intestine. However, when embryos were exposed to 10 ppm PFOS, elevated ROS production was also observed within the liver and brain region, as well as the exposed epidermis. This observation is consistent with previous studies that have identified both induction of oxidative stress (Du et al., 2017; Huang et al., 2022; Sant et al., 2018; Shi & Zhou, 2010) including ROS, and targeting of both liver and brain (Cheng et al., 2016; Cui et al., 2017; Du et al., 2009; Huang et al., 2010; Wu et al., 2022), by PFOS in the zebrafish embryo model. The targeting of hepatocytes and brain as reflected by increased ROS production is, in turn, aligned with several of the alterations in metabolic profiles observed in PFOS-exposed zebrafish that identified both relevant *tissue-specific* metabolites, and several metabolites associated with detoxification and energy metabolism, as primary functions of the liver, in particular, as well as metabolites associated with oxidative stress and related mechanisms of toxicity (as discussed in the section *Integrated cellular model of PFOS toxicity*).

Metabolomic and lipodomic profiles of embryos exposed to PFOS

For both exposure groups, the same 39 metabolites were effectively resolved and subsequently quantified from HRMAS

FIGURE 1: Dose-dependent embryotoxicity of perfluorooctane sulfonic acid (PFOS) for zebrafish embryos exposed at 24 to 96 and 72 to 96 hpf. Toxicity was measured as percentage lethality (% lethality), and presented relative to log (PFOS), ppm. Also given are the associated median lethal concentrations (LC50s) for each exposure window.
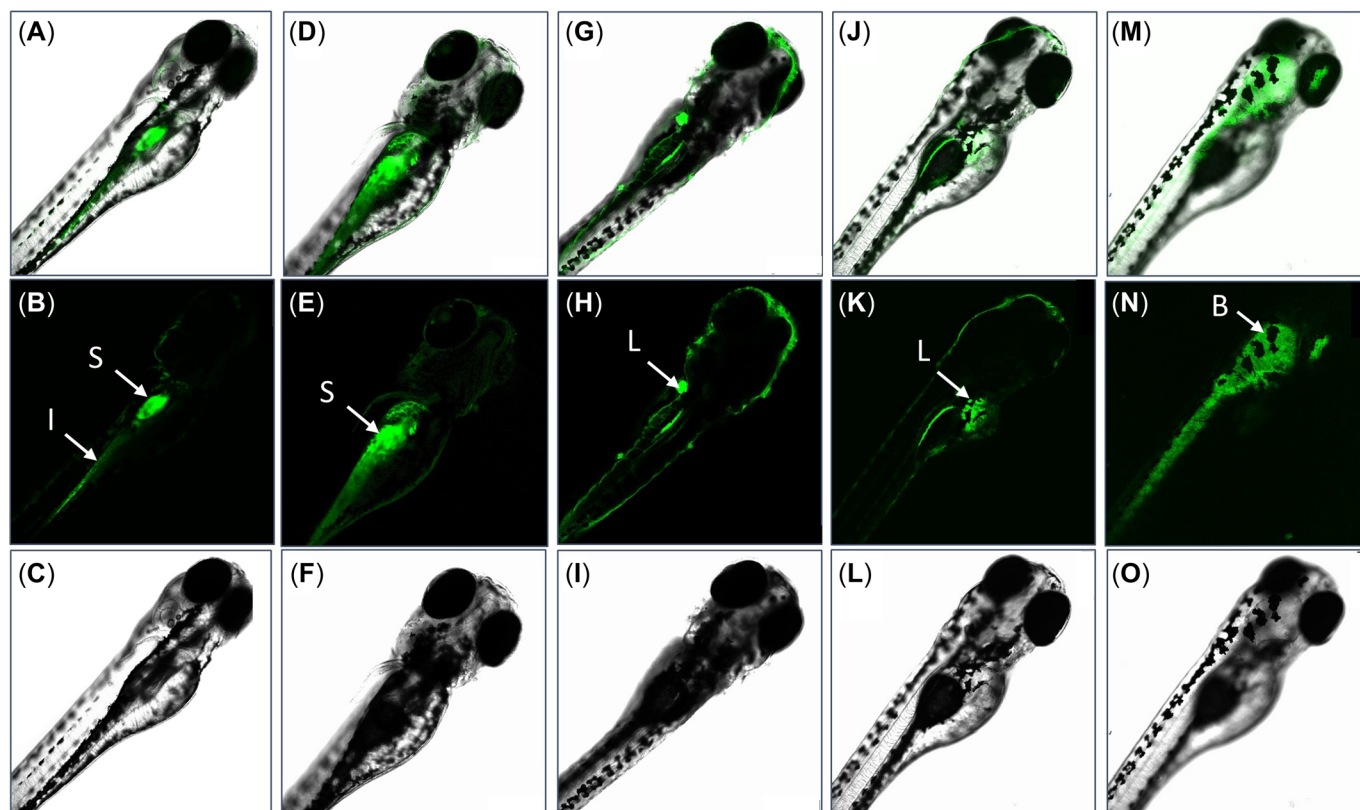
FIGURE 2: In vivo fluorescence detection of reactive oxygen species (ROS) in zebrafish embryos exposed to perfluorooctane sulfonic acid (PFOS; 10 ppm) at 72 hpf for 24. Production of ROS was detected using intracellular fluorescein-based probe with imaging by light and fluorescence confocal microscopy. Shown are light micrographs (bottom row), fluorescence micrographs (middle row), and composite images (top row). Fluorescence indicative of ROS was detected in the GI tract including stomach (S) or intestine (I) of both untreated (**A–C**) and vehicle, that is, 0.001% dimethylsulfoxide (DMSO), only controls (**D–F**), whereas fluorescence (indicative of ROS) was exclusively detected in the liver (L) and brain (B) region, as well as epidermal tissues, of PFOS-treated embryos (**G–O**).

NMR spectra (Figure 3 and Supporting Information S1, Figure S1). Principal components analysis and univariate statistical analyses revealed significant differences between treated and control embryos for both exposure time periods (Figure 4). For the 24 to 96-hpf exposure embryos, 21 metabolites were significantly altered (10 increased, 11 decreased), whereas, for zebrafish exposed over the 72 to 96-hpf period, only 19 metabolites were significantly different from control groups (8 increased, 11 decreased). Of these metabolite alterations, 18 were found to be consistently altered (i.e., increased or decreased) for both exposure periods, whereas lactate (Lac), aspartate (Asp), and carnitine (Carn) were found to only be increased in the 24 to 96-hpf group, and N-acetylaspartate (NAA) was only significantly increased in the zebrafish exposed from 72 to 96 hpf (Figure 4).

Given that both the present study (as discussed in the following text) and previous research (see Gebreab et al., 2020) indicate that PFAS may affect lipids (and their consequent hydrolytic products) as components of cellular membranes, as well as lipid metabolism, a nontargeted, LC–MS lipodomic analysis was conducted. Lipid analysis identified and quantified more than 200 lipids (Supporting Information S1, Table S1). Statistical analyses of *annotated* lipids identified, in particular, significantly reduced levels of 16 DGs (53% of the total number) and increased levels of four cholesteryl esters (CEs; 80% of the total), in PFOS-exposed embryos compared with the control group (Figure 5). In addition, significantly increased levels of 3 (of 37 annotated) phosphatidyl cholines (PCs) and 1 (of 5 annotated) ceramides (Cers) were observed for PFOS-treated embryos (Supporting Information S1, Table S1). No significant differences were observed for any of the triglycerides (50 in total) or lysophosphatidylcholines (5 in total) identified.

Integrated cellular model of PFOS toxicity

Previous studies have explored the toxicity of PFOS using zebrafish, and particularly embryonic and larval stages, as both *model system* and *ecological receptor* (Christou et al., 2020; Huang et al., 2010; Shi et al., 2009). The present study expands on these findings by investigating PFOS embryotoxicity with respect to metabolic changes (at two different developmental stages including pre- and posthatch embryos), and utilized these observable effects, in turn, to develop an integrated cellular model for PFOS toxicity in the zebrafish embryo model (Figure 6). To elucidate pathways associated with PFOS toxicity, as part of this proposed model, the present study primarily employed an HRMAS NMR-based metabolic profiling approach (Figures 3 and 4 and Supporting Information S1, Figures S1), supplemented by a nontargeted LC–MS lipidomics
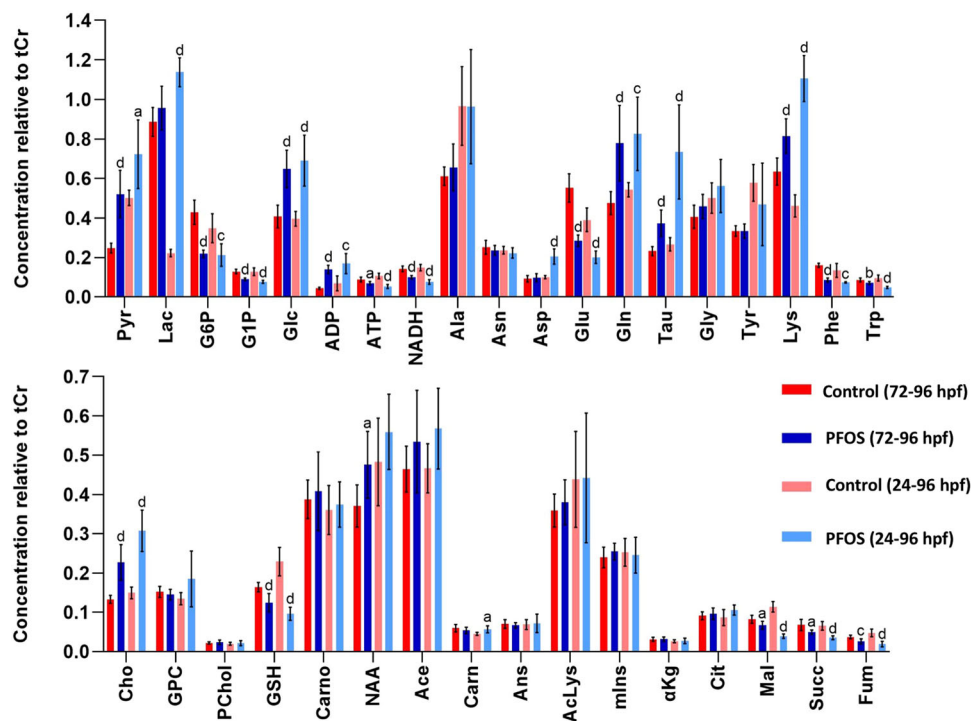
FIGURE 3: Measured levels of metabolites resolved by high-resolution magic angle spinning nuclear magnetic resonance (HRMAS NMR) in zebrafish. Shown are mean levels (±SD), normalized relative to total creatine (tCr; creatine and phosphocreatine), for vehicle only, that is, 0.01% dimethylsulfoxide (DMSO), Control embryos, and embryos exposed to perfluorooctane sulfonic acid (PFOS) at 24 hpf (24–96 hpf) and 72 hpf (72–96 hpf). Statistical significance of difference is indicated with letters as follows: a, $p < 0.05$; b, $p < 0.01$; c, $p < 0.005$; d, $p < 0.001$. Ace = acetate; Ala = alanine; AcLys = acetyllysine; ADP = adenosine diphosphate; aKG = α-ketoglutarate; Ans = anserine; Asn = asparagine; Asp = aspartate; ATP = adenosine triphosphate; Carn = carnitine; Cho = choline; Cit = citrate; G6P = glucose-6-phosphate; G1P = glucose-1-phosphate; Glc = glucose; Gln = glutamine; Glu = glutamate; Gly = glycine; GPC = glycerophosphorylcholine; GSH = reduced glutathione; Lac = lactate; Lys = lysine; Mal = malate; mIns = myo-inositol; Naa = N-acetylaspartate; NADH = reduced nicotinamide adenine dinucleotide; PChol = O-phosphocholine; Phe = phenylalanine; Pyr = pyruvate; Succ = succinate; Tau = taurine; TMAO = trimethylamine-N-oxide; Trp = tryptophan; Tyr = tyrosine.

analysis (Figure 5), and evaluation of oxidative stress (i.e., ROS production; Figure 2). This approach identified significant changes in metabolites associated with a variety of inter-related pathways and associated biological processes, including hepatotoxicity, oxidative stress response, mitochondrial dysfunction, and energy metabolism (Figure 3).

It has been previously shown that PFOS primarily accumulates in tissues with high protein content including, in particular, the liver—a primary target organ—of fish (e.g., rainbow trout, Martin et al., 2003; carp, Hagenaars et al., 2008). Several studies have also demonstrated that the uptake of PFOS into cells and its distribution in tissues are facilitated by certain solute carrier (SLC) transporters that are, likewise, predominantly found in the liver and kidney (Popovic et al., 2014; Yang et al., 2010). Concomitantly, several previous reports in fish including rainbow trout (*Oncorhynchus mykiss*), fathead minnow (*Pimephales promelas*), and white sucker (*Catostomus commersoni*) have demonstrated altered liver function, as indicated by increases in hepatic fatty acyl-CoA oxidase activity and oxidative damage, with PFOS as a key component of such toxicity (Oakes et al., 2005).

In the present study, targeting of the liver is suggested by apparent ROS production (as observed by fluorescent localization) in the liver (Figure 2). Moreover, both the targeting of hepatocytes by PFOS, and the role of oxidative stress, are suggested by the decreased levels of *reduced* glutathione (GSH); not only is GSH associated with oxidative stress, as a key antioxidant for removal of ROS, but enriched (albeit not exclusively located) in the liver as part of Phase II detoxification pathways, that is, conjugation of xenobiotics (Franco et al., 2020). Further aligned with targeting of the liver by PFOS, increased levels of lysine (Lys) were observed in exposed zebrafish; the catabolism of Lys via the *saccharopine pathway* primarily occurs in hepatocytes, specifically in hepatic mitochondria (Higgins et al., 2005), and the observed increase may suggest that the ability to catabolize this amino acid may be inhibited by hepatocellular dysfunction including, in particular, mitochondrial impairment (as discussed in the following text). Altered levels of other amino acids that are also primarily catabolized in the liver including glutamine (Gln) via glutamate (Glu), Asp, and aromatic amino acids may similarly reflect toxicity toward hepatocytes, as well as a role in mitochondrial impairment. In parallel, increased levels of *free* Carn, essential to the "carnitine shuttling" of fatty acids to the mitochondria, as part of the catabolic β-oxidation that primarily occurs in the liver, further point to impaired liver function by PFOS. Notably, trimethylamine N-oxide (TMAO), which has been previously proposed as a biomarker for hepatocyte viability in the zebrafish embryo model, was not significantly changed in PFOS-exposed embryos. A similar nonsignificant change in TMAO was, in fact, observed in PFOA-exposed zebrafish
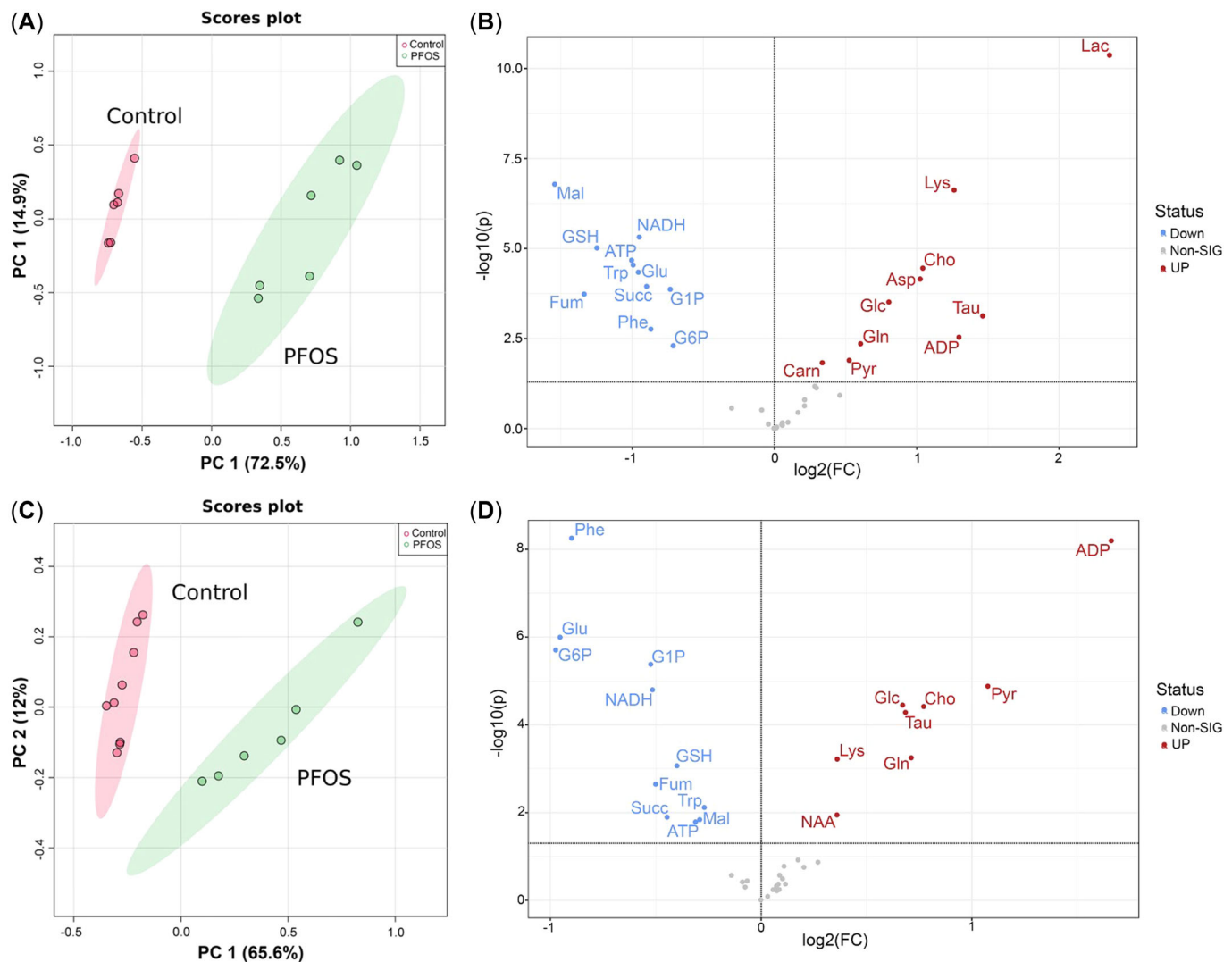
FIGURE 4: Score plots for principle components analysis (PCA), and corresponding volcano plots, showing significant difference in metabolite concentrations (as measured by high-resolution magic angle spinning nuclear magnetic resonance [HRMAS NMR]) of perfluorooctane sulfonic acid (PFOS) treated versus control (0.001% dimethylsulfoxide [DMSO] only) embryos at 96 hpf exposed at either 24 hpf (**A** and **B**) or 72 hpf (**C** and **D**). Score plots (**A** and **C**) show PFOS-exposed (green) versus control (pink) embryos for both exposure times, indicating significant differences in multivariate analyses. Volcano plots (**B** and **D**) show log fold-change (*FC*) in the metabolite on the x-axis, as either an increase (red, more than 0), or a decrease (blue, less than 0), or no significant change (gray) relative to control, and level of significance (as −log *p* value) on the y-axis with minimal significance level ($p < 0.05$) shown as a solid line. For abbreviations of metabolites, see Figure 3 legend.

embryos also exposed at 72 hpf (and measured by HRMAS NMR; Gebreab et al., 2020), suggesting perhaps that whereas PFOS (and PFOA) may target hepatocytes, it is not *hepatocytotoxicity*, that is, cell death, but rather impairment of hepatocyte *function*, that underlies embryotoxicity.

In addition to apparent targeting of liver (based on ROS production and metabolite profiles), increased ROS production was observed in the brain region of PFOS-exposed embryos, consistent with previous studies that have suggested neuro-toxicity of PFAS including PFOS in the zebrafish embryo model (Gaballah et al., 2020; Gebreab et al., 2020; Lee et al., 2021). Further supporting targeting of the central nervous system (CNS), a significant increase in the neuron-specific metabolite, NAA was observed in 72-hpf embryos exposed to PFOS, sug-gesting impacts on neuronal and/or glial function at this later stage of development.

Alongside apparent targeting of hepatocytes and neural cells by PFOS, metabolic changes and related observations specifi-cally point to a role of oxidative stress in embryotoxicity, as has been previously reported in experimental systems including zebrafish (Du et al., 2017; Huang et al., 2022; Sant et al., 2018; Shi & Zhou, 2010). As previously mentioned, PFOS-exposed embryos showed increased ROS production in the developing liver, and at the same time a significant decrease in GSH, as a key antioxidant (and Phase II detoxifying) metabolite, was observed. A decrease in GSH has been generally connected to changes in oxidative stress levels, because GSH takes part in the conversion of hydrogen peroxide to water within biological systems; the induction of oxidative stress by PFOS has also been noted in previous studies (Hagenaars et al., 2008; Liu et al., 2007). In addition, an observed increase in the levels of taurine (Tau) in PFOS-exposed zebrafish may also indicate a response to
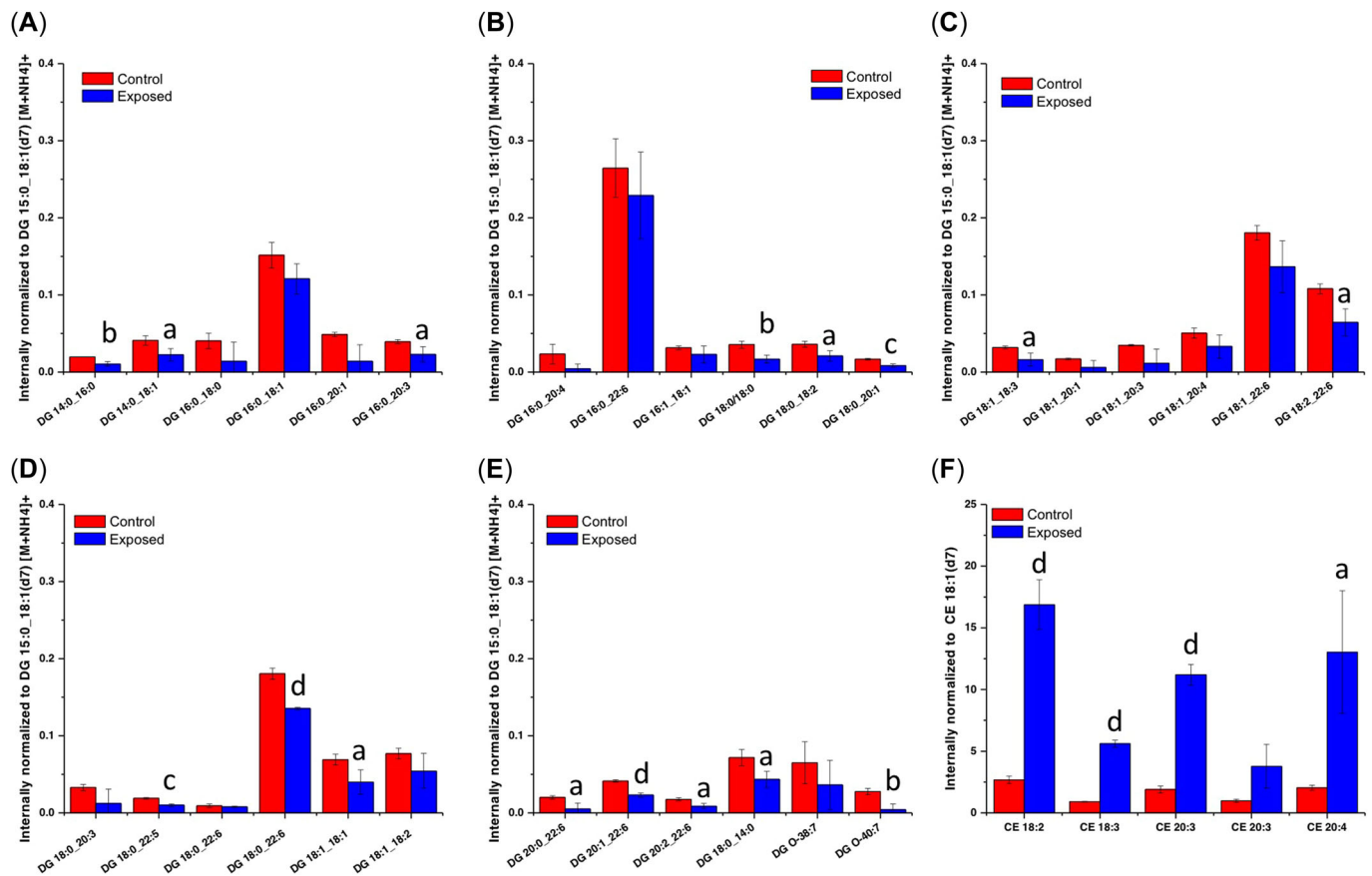
FIGURE 5: (A–F) Alterations of diglycerides (DG) and cholesteryl esters (CE), measured in liquid chromatography–mass spectrometry lipidomic studies, as the two most prominently affected classes of lipids. Given for each are length and unsaturation of acyl groups. For additional results of lipidomic studies, see the Supporting Information S1, Table S1. Statistical significance of differences is indicated with letters as follows: a, $p < 0.05$; b, $p < 0.01$; c, $p < 0.005$; d, $p < 0.001$.

oxidative stress, because Tau has a well-established role in antioxidant defense (Schaffer et al., 2009; Sun et al., 2018).

The ability of PFOS to induce oxidative stress, as well as other aspects of its cellular toxicity, is thought to result from an interaction with a number of transcription factors. It has, for example, been shown that PFOS inhibits *silent information regulator 1* (SIRT1) activity, specifically through binding of the nicotinamide adenine dinucleotide (NAD+) binding cavity (Duan et al., 2021) which is imperative for deacetylase activity (Kalous et al., 2016). Activated SIRT1 deacetylates a wide range of substrates including the transcription factors nuclear factor erythroid 2–related factor 2 (NRF2) and peroxisome proliferator-activated receptor (PPAR), which have vital roles in lipid metabolism, oxidative stress, and inflammation (Dovinova et al., 2020; Kaspar et al., 2009; Kim et al., 2010), and that have been previously linked to the toxicity and other adverse impacts (e.g., metabolic impairment) of PFOS. Deacetylation of NRF2 by SIRT1, in particular, promotes the transport of the transcription factor to the nucleus, where it interacts with the antioxidant response element (ARE) to mediate the transcription of its target genes including *heme oxygenase 1* (HO-1), *superoxide dismutase 1* (SOD1), and *glutathione peroxidase* (GPx) that are vital to controlling the oxidative environment (Xu et al., 2021). In addition, it has been previously reported that PFOS can induce

phosphorylation and degradation of the nuclear factor κB (NF-κB) inhibitor α (IκBα), which regulates the translocation of NF-κB from the cytoplasm to the nucleus, and results in the transcription of pro-inflammatory cytokines (Chen et al., 2018). Therefore, inhibition of SIRT1 activity and induction of NF-κB signaling pathways may partially contribute to the oxidative stress induced by PFOS (as evidenced by elevated ROS), and consequent alterations in metabolic profiles (e.g., decreased GSH, increased Tau) in exposed zebrafish.

Deleterious effects of PFOS-induced oxidative stress have been noted in a number of both in vitro and in vivo fish model systems, whereby accumulation of ROS can damage a variety of cellular organelles including, in particular, mitochondria. Impaired mitochondrial function includes decreased adenosine triphosphate (ATP) production through the opening of the mitochondrial permeability transition pore (MPTP), and disruption of other crucial processes leading to cell death (Kowaltowski et al., 2001). Consistent with mitochondrial damage, observed increases in choline (Cho), as a hydrolytic product of cell membrane disruption, in the present study may indicate compromise of mitochondrial, or perhaps other cellular, membranes: choline is, in particular, the polar head group associated with phosphatidylcholines, which are the most abundant phospholipids founds in mitochondrial membranes
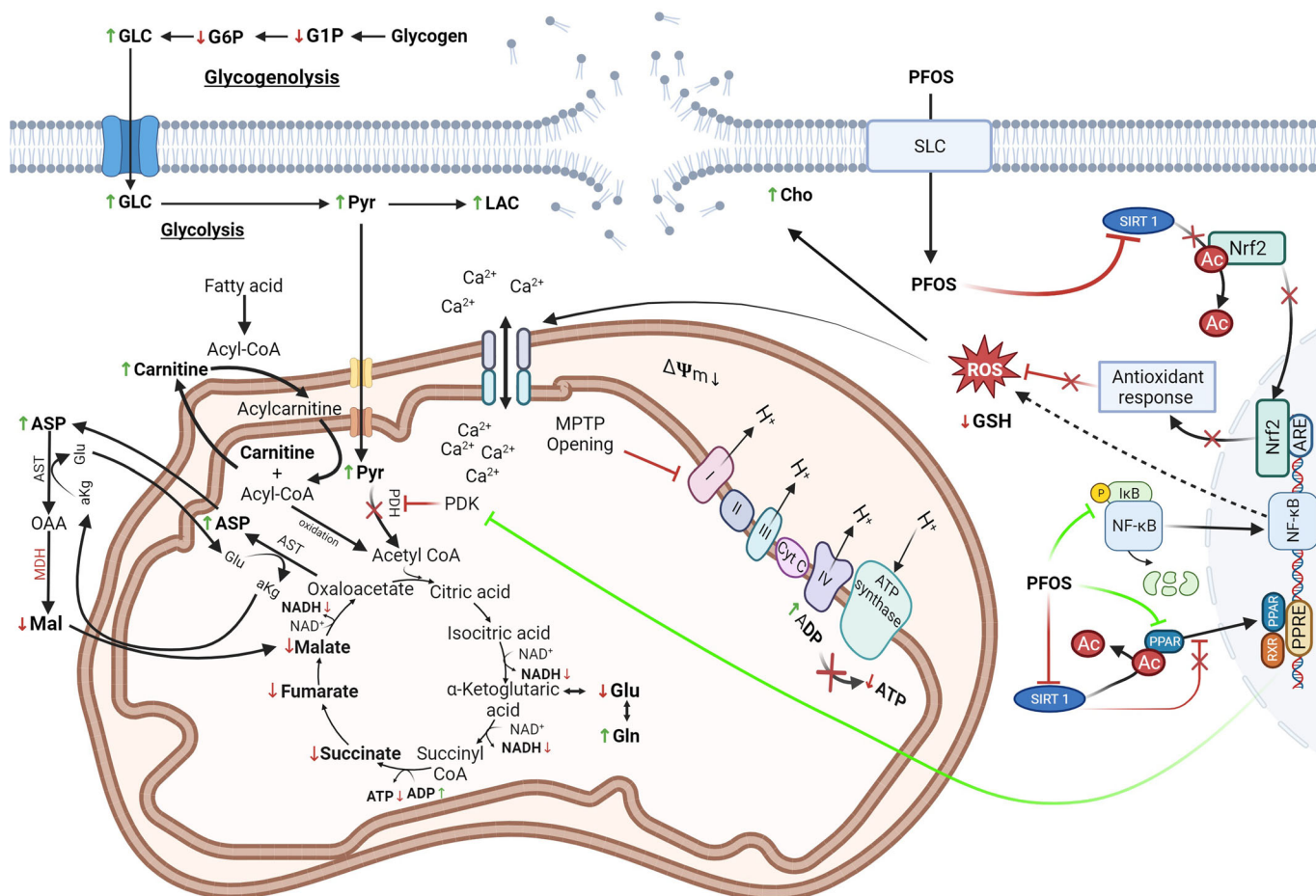
FIGURE 6: Integrated model of perfluorooctane sulfonic acid (PFOS) toxicity in the zebrafish embryo model. Metabolites measured by high-resolution magic angle spinning nuclear magnetic resonance (HRMAS NMR) are indicated by corresponding green upward arrows (↑) and red downward arrows (↓) indicating increase and decrease, respectively. Uptake and tissue distribution of PFOS is facilitated by SLC transporters that are predominantly found in the liver. Once inside the cell, PFOS disrupts redox status through 1) inhibiting the deacetylation capability of sirtuin 1 (SIRT1), and thus its ability to activate nuclear factor erythroid 2-related factor (NRF2) that promotes the transcription of antioxidant response elements; and 2) through inducing phosphorylation and degradation of nuclear factor κB (NF-κB) inhibitor α (IκBα), which regulates the translocation of NF-κB that results in the transcription of pro-inflammatory cytokines (as evidenced by decreased glutathione [GSH]). Oxidative stress due to increased reactive oxygen species (ROS) can impact cellular membranes via lipid peroxidation leading to hydrolysis of phospholipids, as evidenced by increased choline (Cho), and damage to mitochondrial membranes through induced opening of the mitochondrial permeability transition pore (MPTP). Opening of the MPTP can lead to the disruption of oxidative phosphorylation via disruption of the mitochondrial membrane potential, leading to disrupted adenosine triphosphate (ATP) production. In addition, PFOS also can induce PPARα activation both directly, and indirectly through inhibition of SIRT1 deacetylation of peroxisome proliferator-activated receptor (PPAR), leading to the transcription of pyruvate dehydrogenase kinase 4 (PDK4), and subsequent inhibition of pyruvate dehydrogenase (PDH) for entry of pyruvate (Pyr) into the Krebs cycle, leading to increased Pyr levels. Downstream, decreased Pyr input into the Krebs cycle can lead to disruption to mitochondrial energy metabolism evidenced by decreased Krebs cycle intermediates including Fum, Succ, and Mal, and reduced nicotinamide adenine dinucleotide (NADH). Disruption of mitochondrial function, and the Krebs cycle can affect auxiliary pathways such as the conversion of glutamate (Glu) into α-ketoglutarate (αKG), and the shuttling of fatty acids into the mitochondria as acylcarnitine for β-oxidation. In addition, PFOS is known to modulate enzymes of the Mal-Asp shuttle, and specifically, aspartate transaminase (AST) and malate dehydrogenase (MDH), which transport reducing equivalents from glycolysis to the Krebs cycle. Upstream, impacts of Krebs cycle dysfunction include changes in carbohydrate metabolism including increases in Glc, and decreases in glucose-1-phosphate (G1P) and glucose-6-phosphate (G6P), potentially indicating an increase in glycogen breakdown to meet energy requirements. In parallel, due to decreased flux of Pyr into the Krebs cycle, an increase in Lac was observed, as a presumptive means to provide NADH (and reducing equivalents for the Krebs cycle) through anaerobic glycolysis. For substances not defined, see Figure 3 legend.

(Schuler et al., 2016). Significant increases in Cho are consistent with both previously reported disruption of cellular membranes by PFOS (Lehmler et al., 2006; Xie et al., 2010), in general, and specifically, similar observations of increased Cho in relation to mitochondrial membrane disruption by analogous PFAS including PFOA (Gebreab et al., 2020).

Aligned with a proposed disruption of mitochondria, several metabolites associated with mitochondrial function including

the Krebs cycle, and associated production of ATP via oxidative phosphorylation, as well as catabolism of amino acids and fatty acids (i.e., "carnitine shuttle"), and energy metabolism more generally, were altered in PFOS-exposed embryos. This is not surprising given that mitochondrial dysfunction has been previously linked to the oxidative stress induced by PFAS (Zhao et al., 2011). In the present study, significant decreases were observed for malate (Mal), fumarate (Fum), and succinate

(Succ), as components of the Krebs cycle, suggesting impairment of this key mitochondrial function that specifically generates reduced nicotinamide adenine dinucleotide (NADH), as a source of protons, for generating ATP via oxidative phosphorylation. Indeed, decreased NADH levels, as well as reduced levels of ATP (and concurrently, increased adenosine diphosphate [ADP]), were observed. Although reductions in NADH (from the Krebs cycle) may partly explain concurrent decreases in ATP, it has been previously suggested (and proposed in our study; Figure 6) that PFOS may, in addition, directly interfere with ATP production via disruption of mitochondrial membranes including, in particular, opening of the MPTP, as an integral component of oxidative phosphorylation (Khansari et al., 2017).

Alongside alterations in Krebs cycle intermediates, and subsequent production of ATP, several metabolites associated with auxiliary pathways including, in particular, the amino acid and fatty acid metabolism that supplies intermediates for the Krebs cycle. were also altered in PFOS-exposed embryos. Glutamate and glutamine, for example, are vital to the function of the Krebs cycle: cytosolic Gln is transported to the mitochondria, and converted to Glu (by glutaminase), which,in turn can be converted to α-ketoglutarate (αKG; Yoo et al., 2020). The observed increase in Gln, and decrease in Glu, would be consistent with disruption of mitochondria, and consequently, the Krebs cycle. At the same time, however, the decrease in Glu levels may reflect disruption to the "malate-aspartate shuttle" (which transports Mal into mitochondria), because a concurrent increase in Asp, and a decrease in Mal, was also observed in PFOS-exposed fish. Altered levels of aspartate aminotransferase (AST), which produces Glu via transamination in the conversion of Asp to Mal (for subsequent transport into mitochondria to supply the Krebs cycle), has been previously proposed as part of the cellular toxicity of PFAS, and also, has been noted as a biomarker of hepatic injury (Borghese et al., 2022). Also, decreased levels of malate dehydrogenase (MDH) have been observed in the gills of European bullhead (*Cottus gobio*) after exposure to 1 ppm of PFOS (Dorts et al., 2011); these decreased levels may thus similarly explain the observed changes in levels of Glu, Asp, and Mal, because MDH is responsible for the conversion between Mal and oxaloacetate during the Mal–Asp shuttle. In addition to glutamate metabolism, the observed increase in Lys, as an essential amino acid, suggests reduced catabolism of this amino acid, and most likely, impairment of the saccharopine pathway, which is confined to the mitochondria, primarily the mitochondria of hepatocytes. Likewise, apparent changes in the catabolism of aromatic amino acids may reflect reduced energy-producing capacity of mitochondria (and support of auxiliary pathways). An observed decrease in the *essential* aromatic amino acids phenylalanine (Phe) and tryptophan (Trp), although *not* tyrosine (Tyr), is consistent with impairment of mitochondria because both tyrosine hydroxylase (i.e., hydroxylation of Phe to Tyr) and tryptophan aminotransferase—the first, committed and/or rate-limiting steps in the catabolism of Phe and Trp, respectively—occur in the cytosol, whereas Tyr aminotransferase (the first step in the catabolism of Tyr) has

both cytosolic and mitochondrial forms. Accordingly, it is proposed that decreased Phe and Trp (and, specifically, removal by corresponding catabolic enzymes, that is, Tyr hydroxylase and Trp aminotransferase) reflects increased catabolism of these amino acids as a compensatory mechanism to offset reduced mitochondrial energy production including catabolism of other amino acids (e.g., Glu/Gln, Lys, Asp) and fatty acids. The altered metabolism of amino acids and the increased levels of Carn (Figures 3 and 4) may likewise suggest disruption of mitochondria, and consequent impairment of energy production. Carnitine is an essential cofactor for the transportation of fatty acids such as acylcarnitines into mitochondria for β-oxidation (producing acetyl CoA and NADH). Increased Carn suggests altered, and perhaps increased β-oxidation of fatty acids, as has been previously suggested for PFOA in similar metabolomics studies in the zebrafish embryo (Gebreab et al., 2020; Figure 6).

Upstream of the mitochondrial pathways, HRMAS NMR profiles (Figure 3) suggest alteration by PFOS of carbohydrate metabolites including increased glucose (Glc), and concurrent decreases in both glucose-1-phosphate (G1P) and glucose-6-phosphate (G6P), as well as increased pyruvate (Pyr), most likely due to reduced uptake and utilization by mitochondria (i.e., the Krebs cycle). These observations, generally speaking, suggest modulation of carbohydrate metabolism (Figure 6) either indirectly, in response to PFOS impacts on mitochondrial energy metabolism, or perhaps directly through one or more molecular mechanisms previously associated with PFOS (e.g., PPAR; discussed in the next paragraph). Analogously, PFOA has been previously shown to alter glucose metabolism in zebrafish (Hagenaars et al., 2013), and other model systems (e.g., mouse; Zheng et al., 2017). Perhaps most telling, G1P is almost exclusively associated with glycogen metabolism including synthesis (i.e., glycogenesis), and breakdown to supply glucose (i.e., glycogenolysis); thus the reduced levels of G1P, alongside increased Glc, strongly suggest either upregulated glycogenolysis, as a means of increasing Glc availability, or downregulated glycogenesis, as a compensatory mechanism in light of impaired energy (i.e., ATP) production in PFOS-exposed embryos. Previous studies of the carboxylic acid analog, PFOA, in fact, have suggested the diversion of glycogen toward glucose, as a presumptive means of compensating reduced energy metabolism by mitochondria, in zebrafish embryos (Hagenaars et al., 2013). Likewise, in vivo and ex vivo studies of mice have measured decreased glycogen in response to PFOS (Wan et al., 2021; Wang et al., 2014).

On the other hand, G6P is associated with both glycogen and glucose metabolism, including in the latter case both glycolysis (supplying Pyr for mitochondrial energy production), and the synthesis of Glc (i.e., gluconeogenesis). Thus decreased G6P may either similarly reflect diversion of glycogen stores toward production of Glc (as suggested by decreased G1P), or alternatively, consumption of this intermediate as part of either glycolysis (toward mitochondrial energy production), or de novo synthesis of Glc. At the same time, an increase in Lac was also observed, exclusively for embryos exposed at 24 hpf, and may suggest diversion of elevated Pyr (due to

mitochondrial impairment) to anaerobic glycolysis, as a compensatory mechanism for producing ATP, in the absence of oxidative phosphorylation over this extended exposure time.

Providing possible insights regarding the pathway(s) responsible for observed alterations in energy metabolism, PFAS including PFOS have been shown to activate PPAR, a key regulator of several pathways of energy metabolism including, in particular, glucose and lipid metabolism (Rosen et al., 2017). It has been shown that PFAS can transactivate PPAR, and in particular, PPARα and PPARγ, which have in turn been shown to regulate glycolysis, gluconeogenesis, and glycogen metabolism (Peeters & Baes, 2010), as well as numerous aspects of lipid and lipoprotein metabolism including β-oxidation; indeed, fatty acids are agonistic ligands of PPAR (Gervois et al., 2000).

In addition, it has been shown (Kosgei et al., 2020) that PPAR is a substrate for deacetylation by SIRT1, which is in turn inhibited by PFOS (Duan et al., 2021), suggesting that PFOS can, at the same time, indirectly activate PPAR through dysregulation. Accordingly, a role in the transactivation of PPAR by PFAS, and specifically, PFOA and chemically related perfluoroether carboxylic acids (PFECAs), has been previously implicated in similarly altered metabolic (carbohydrate in particular) profiles in the zebrafish embryo model (Gebreab et al., 2020). Most notably, PPAR has been shown to both upregulate gluconeogenesis (Im et al., 2011), and downregulate glycolysis (Oosterveer et al., 2009). A role of PPAR regulation in glycogen metabolism, on the other hand, remains to be clarified; despite decreased glycogen induced by PPARα agonists (such as PFAS), the only data currently available suggest *upregulation* of glycogen synthase, the rate-limiting step in glycogen synthesis, by PPAR (Peeters & Baes, 2010). The postglycolytic fate of energy factors such as Pyr is more clearly affected by PPARα, because pyruvate dehydrogenase kinase 4 (PDK4) transcription is stimulated by PPARα activation (Wu et al., 2001), and in turn, PDK4 phosphorylates and inactivates pyruvate dehydrogenase (PDH), the enzyme needed to convert pyruvate to acetyl-CoA. Thus PFOS-induced PPAR activation may explain not only the observed changes in Pyr due to the inhibition of PDH, but also the observed increase in Lac, resulting from metabolic redirection to provide ATP by *anaerobic* means, because the lack of Pyr entry into the Krebs cycle (evidenced by lower Krebs cycle metabolites) would decrease the ATP from oxidative processes (i.e., oxidative phosphorylation). Taking these notions together, it is proposed that activation of PPAR by PFOS either directly or indirectly (e.g., inhibition of deacetylation by SIRT1) modulates carbohydrate and associated aspects (e.g., lipid) of energy homeostasis in unison with otherwise impaired (i.e., mitochondrial) energy metabolism (Figure 6).

To evaluate the potential impact of PFOS on lipid profiles in relation both to the possible disruption of cell membranes and to the role of PPAR (with lipids representing endogenous ligands, and which is, in turn, involved in lipid homeostasis), a nontargeted lipidomic analysis was conducted (Figure 5). Significant changes in a relatively small number of PCs (3 of 37 measured) and Cers (1 of 5 measured) were observed. In the case of the increase in PCs, it is plausible that this change

perhaps reflects the previously reported ability of PFOS, and other PFAS, to disrupt the phospholipid bilayer of membranes (Lehmler et al., 2006; Xie et al., 2010), for which PC, along with TG and cholesterol, are the most abundant lipids (Fraher et al., 2016). Counter to this observation, however, a very recent lipidomics study of zebrafish embryos exposed to PFOS specifically identified, in contrast, consistent *decreases* among numerous PCs (Yang et al., 2023), which would perhaps be more consistent with proposed phospholipid hydrolysis following membrane disruption (Figure 6), as suggested by increased Cho (Figure 3). Notably though, these previous studies utilized *microinjection* of PFAS into the vegetal pole—and thus yolk cells—of very early (i.e., ~2-hpf) embryos, in contrast to the ambient exposure at 72 hpf of the present study; furthermore, it has been shown that PCs become considerably depleted in the yolk, which is a primary source of this lipid, by 72 hpf while at the same time concentrations throughout the developing body reach a maximum at this stage (Fraher et al., 2016). Thus this observational difference may represent a stage-specific difference in lipid profiles. Similarly, the observed decrease in Cer observed in the present study contrasts with previous studies that have reported increases in both PFOS-exposed zebrafish embryos (Yang et al., 2023), and other systems (e.g., mice; Deng et al., 2022), although in these cases, the observed modulation of these lipids was also interpreted as an indicator of altered energy metabolism including metabolic syndrome. Alternatively, the alterations in PC and Cer may both reflect a role of sphingomyelinase, which cleaves the sphingomyelin found in cellular membranes (in particular the myelin sheaths of neurons) to generate phosphocholine, as a key precursor of PC biosynthesis, and Cer, both of which play a role (along with its subsequent cleavage product, sphingosine) as signaling lipids in a wide range of cellular processes. Indeed, previous studies have implicated sphingomyelin metabolism in the adverse effects of exposure to PFOS, and other PFAS (Seyoum et al., 2020; Prince et al., 2023; Rhee et al., 2023). Given the relatively small number of PCs and Cers affected by PFOS exposure in the present study, however, it is unclear how much any of these (or other mechanisms) may contribute to the observed toxicity, and associated metabolic alterations, in the zebrafish embryo model. In contrast, however, to the relatively small number of PCs and Cers altered by PFOS, significant changes were observed for a majority of both DGs (16 of 30 measured) and CEs (4 of 5 measured).

Observed alterations in DGs were not only considerably more prevalent (Figure 5), but are also consistent with previous lipidomics studies of PFOS in zebrafish embryos that also reported consistently significant decreases in levels of these lipids (Yang et al., 2023). Interestingly, these previous studies delineated a difference, in this regard, between PFOA and PFOS, whereby the former consistently increased DG levels, suggesting a difference between congeners. Notably, no significant change was observed for any of the 50 annotated TGs measured; this contrasts with previous lipidomic studies that consistently showed significant decreases in TG in PFOS-exposed zebrafish embryos (Yang et al., 2023). Again, however, these previous studies were done via microinjection of very

early (2-hpf or less) embryo stages, and it has been shown that although yolk-derived TGs are largely depleted by 72 hpf, DG levels in the developing body of the embryo reach a maximum at this stage (Fraher et al., 2016). Furthermore, whereas TGs primarily function in the storage and transportation of fatty acids, membrane-bound DGs participate in the regulation of a number of cellular functions, particularly through activation of protein kinase C (PKC), which in turn regulates (via phosphorylation) a wide range of targets including the NF-κB pathways that have been implicated as a target in PFAS toxicity (Chen et al., 2018; discussed in the previous section, *Integrated cellular model of PFOS toxicity*). Moreover, PFOS (and other PFAS) are well-established agonists of PPAR; an interaction between PPAR and lipid homeostasis including, in particular, metabolism of the fatty acids DG and TG has been shown in numerous studies. Specifically, it has been shown that other agonists of PPARγ also reduce levels of DG (Liu et al., 2011; Verrier et al., 2004). In addition, overexpression of diglyceride acyltransferease (DGAT), the enzyme that catalyzes the formation of TG from DG, can rescue the toxicity and associated increase in DG and free fatty acids in mice overexpressing PPARγ (Liu et al., 2012), whereas DGAT knockout mice showed reduction in several PPAR and downstream pathways (Liu et al., 2011), suggesting cross-talk between PPAR and DG metabolism, and specifically coordinated regulation of DGAT and PPAR. At the same time, metabolic profiling—specifically, increases in Carn (Figure 3)—suggests altered, and possibly increased, β-oxidation of fatty acids (Figure 6), which may additionally contribute to reduced levels of DG; activation of PPAR has, in fact, been shown to increase β-oxidation. The observed decrease in the majority of DGs in PFOS-exposed zebrafish embryos may therefore suggest a role of these inter-related pathways of fatty acid and glycerolipid metabolism in the toxicity, and associated metabolic alterations, observed in the present study.

Similarly, among the five cholesteryl esters (CE 18:2, CE 18:3, CE 20:3, and CE 20:4) quantified during these lipidomic studies, four exhibited significant increases in PFOS-exposed fish, compared with the control group. Cholesteryl esters result from the esterification of cholesterol with long-chain fatty acids, a process initiated by the protein apoA-I, and are essential for facilitating subsequent cholesterol transportation and metabolism via cholesteryl ester transport protein (CETP), particularly with respect to high-density lipoproteins (HDLs; Xu et al., 2022). The observed alterations in CEs in our study align with prior reports of substantial changes in *apoA-I* gene expression levels in PFAS-exposed fish (Bilbao et al., 2010; Cui et al., 2017), as well as other biological systems (Bijland et al., 2011; Zhang et al., 2016), because these changes in *apoA-I* would be expected to alter the degree of cholesterol esterification. Moreover, alterations in CEs coincide with a previously shown role of CETP in metabolic syndrome, and particularly dyslipidemia (Sandhofer et al., 2006). It has been shown that PPAR agonists upregulate CETP, that CETP is in turn inversely correlated with HDL (Beyer et al., 2008), and that CETP inhibition increases HDL (Hansen et al., 2010). It is proposed that the increased CE levels by PFOS, as a recognized

PPAR agonist, might similarly point to dyslipidemia including reduced HDL as characteristic of metabolic syndrome. Interestingly, it has been shown that PFOS can directly bind to apoA-I in fish (Honda et al., 2014), potentially contributing to the accumulation of PFOS; this may represent a PPAR-independent means by which PFOS interferes with cholesterol metabolism and homeostasis. Finally, it is known that apoA-I and CETP are expressed in yolk of zebrafish (Fraher et al., 2016), and can, accordingly, play a role in the development of early life stages of fish—because the transport of lipids from the yolk to the embryo is vital to fish development (Mahoney et al., 2023)—and observed alterations in CEs may thus additionally suggest a mechanism for the observed embryotoxicity.

Biomarkers of PFOS toxicity

Notably, many of the observed effects of PFOS on metabolite profiles mirror patterns previously observed (Gebreab et al., 2020) for zebrafish embryos, similarly evaluated by HRMAS NMR, in relation to its carboxylic acid analog, PFOA. The present study thus extends these previous observations regarding the metabolic impacts of perfluorocarboxylic acids to perfluorosulfonic acid congeners. Despite these similarities, however, a few potentially revealing differences between metabolic profiles of PFOA- and PFOS-exposed embryos, specifically at 72 hpf, in both cases, were also noted (Supporting Information S1, Table S1). It is proposed that these differences may represent potential *biomarkers* for effect; thus exposure to PFOS and its effects are distinct from those of other PFAS.

The majority of these differences between PFOA (Gebreab et al., 2020) and PFOS point to a differential role of PPAR as a recognized target, and consequent intermediary of the effects on metabolism, with respect to the two congeners. At least one study (Takacs & Abbott, 2006) has suggested that PFOA more strongly (than PFOS) transactivates PPAR, and specifically PPARα, in a luciferase reporter assay. Studies (Abbott et al., 2009) have also shown that the developmental toxicity of PFOS, in the mouse model, is not PPAR dependent, whereas PFOA developmental toxicity is, and PFOS has been linked (Ren et al., 2009; Rosen et al., 2010, 2017) to several alternative, PPAR-*independent* pathways including the constitutive androstane receptor (CAR).

This relative dependence on, and consequent role of, PPAR may explain the differences between the effects of PFOS and PFOA in several aspects of their metabolic profiles. Although increases and decreases, respectively, in Glc and G6P concentrations were observed for both PFOA- and PFOS-exposed embryos, no significant effect of PFOA was observed, for example, with respect to G1P (Gebreab et al., 2020), whereas this metabolite was significantly increased in PFOS-exposed embryos (Figure 3). Given the unique association of G1P with glycogenolysis and glycogenesis, it is suggested that relatively higher activation of PPAR, as a known regulator of glycogen synthesis, by PFOA may explain this observed difference, specifically as a metabolic shift toward glycogen *synthesis*—and,

moreover, away from breakdown for PFOA-exposed embryos, resulting in the observed lack of change in G1P (as a key intermediate, and indicator, of glycogenolysis), in contrast to PFOS.

Perhaps one of the most revealing differences between PFOA and PFOS is a lack of significant change, in the case of the former, in the measured levels of ADP, whereas ADP increased significantly in embryos exposed to the latter. It has been suggested that ADP levels are primarily responsible for changes in energy state (Wilson, 2017), and it is known that increased and decreased cytosolic (ATP)/(ADP) determines (via suppression of glycolytic enzymes) whether energy metabolism favors, respectively, mitochondrial pathways, that is, Krebs cycle and oxidative phosphorylation, or glycolysis (Maldonado & Lemasters, 2014). Such a shift is most notably observed in cancer cells, as part of the well-described Warburg effect, whereby proliferating cells transition from ATP production via mitochondria to cytosolic glycolysis. Whereas (ATP)/(ADP) was approximately 1:1 in previous studies of PFOA-exposed embryos (Gebreab et al., 2020), the <1:3 ratio in PFOS-exposed embryos in the present study would be consistent with a metabolic shift toward glycolysis. At the same time, PPAR has been shown to downregulate glycolysis (and upregulate gluconeogenesis), and thus a higher degree of transactivation of PPAR by PFOA, compared with PFOS, could explain (alongside a lack of glycolytic suppression, and disruption of mitochondrial membrane functions) the dichotomy in energy metabolism between the two PFAS congeners.

In turn, it is proposed that a shift to glycolysis in embryos exposed to PFOS, rather than oxidative phosphorylation, accompanies observed differences (compared with PFOA; see Supporting Information S1, Table S1) in several other metabolites including those associated with the Krebs cycle (e.g., Cit, Mal, and Fum), and supporting the Mal-Asp shuttle (i.e., Mal, Asp), and β-oxidation (e.g., Carn, acetate). The latter, furthermore, coincides with a consistently measured decrease (in lipidomics studies) of DG, as previously reported (Yang et al., 2023), which—in contrast to the reported increase of DG in zebrafish embryos exposed to PFOA (Yang et al., 2023)—points to a possible PFOS-specific role of inter-related pathways of fatty acids (i.e., β-oxidation) and glycerolipid metabolism. In addition, although both levels of Phe and Trp were conspicuously found to significantly decrease in PFOS-exposed embryos, all three aromatic amino acids (i.e., Phe, Tyr, and Trp) were significantly *increased* in PFOA-exposed embryos: aligned with this finding, it has been shown in several studies that, aligned with this observation, PPARα downregulates amino acid catabolism (Contreras et al., 2015; Kersten et al., 2001; Tobón-Cornejo et al., 2021).

Although a role of PPAR may explain the differences between PFOS and PFOA with respect to several aspects of metabolic profiles, and represents a potential biomarker for distinguishing exposure, and consequent effect, of the two congeners, other observed differences are not as clear. Most conspicuously, perhaps, is the opposing change in the neural metabolite, NAA, which was significantly increased in PFOS-exposed embryos, and has been previously reported to decrease in PFOA-exposed embryos (Gebreab et al., 2020). In the latter case, the decrease of this metabolite was attributed to possible toxicity toward neural cells, specifically in light of observed behavioral dysfunctions for PFOA-exposed embryos. In the present study, increased ROS production was observed in the brain region of PFOS-exposed embryos, but the elevated levels of NAA would not be consistent with neural *cytotoxicity*. Instead, NAA has been linked to the interaction between neural and glial cells (Moffett et al., 2007; Xu et al., 2016), including a role in the recycling of Glu between astrocytes and neurons (Patel et al., 2014), and serving as a reservoir for Glu, as a neurotransmitter (Clark et al., 2006). Thereby, increased NAA for PFOS might reflect disruption of neural *function* rather than cytotoxicity, similar to observed effects on hepatocyte function rather than hepatocytotoxicity, as evidenced by a lack of change in TMAO (as discussed in the previous section, *Integrated cellular model of PFOS toxicity*). Regardless of the underlying cause of this difference in NAA, it represents a compelling candidate as a biomarker of PFOS toxicity, particularly in relation to emerging data suggesting neurotoxicity and neurodevelopmental toxicity of PFAS (Foguth et al., 2020; Gaballah et al., 2020).

Finally, the differences in metabolite profiles observed for the two exposure windows (i.e., 24–96 and 72–96 hpf) are worth noting. Although alterations of metabolic profiles by PFOS were largely consistent between the two groups with shared relative changes in 18 metabolites (out of the 39 metabolites measured in both groups), in the case of 4 metabolites, differences were observed between exposure windows. Significant increases in Asp, Carn, and Lac were observed in the 24 to 96-hpf group, whereas no significant change was observed for embryos exposed at 72 hpf. It is posited that these metabolites reflect a more pronounced transition to "alternative" energetic pathways arising from prolonged (72-h) exposure to PFOS including diversion of alternative substrates (via the Mal-Asp shuttle) into the Krebs cycle (i.e., increased Asp), increased utilization of β-oxidation of fatty acids (i.e., increased Carn), and shift to anaerobic glycolysis (i.e., increased Lac). On the other hand, the neural-specific metabolite NAA was only increased in embryos exposed at 72 hpf. In this case, the observed change in this metabolite may simply reflect developmental stage because it is only at approximately 72 hpf that the CNS in the zebrafish embryo is fully developed, and therefore, it is only at this stage of exposure that impacts (such as elevated NAA levels) on neural/glial systems can be observed.

CONCLUSIONS

The present study aimed to assess the biochemical, molecular, and cellular pathways associated with the toxicity of PFOS in zebrafish embryos as a model system for teleost fish, as relevant ecological receptors, with regard to this widespread aquatic contaminant. Dose-dependent toxicity of PFOS and specifically the LC50 values comparable to previous studies were identified. In addition, visualization of ROS production revealed elevated ROS in the GI tract, liver, brain region, and exposed epidermis of PFOS-exposed embryos. These findings

are consistent with previous studies indicating induction of oxidative stress and targeting of the liver and brain by PFOS. Moreover, metabolomic analysis identified significant alterations in metabolites associated with hepatotoxicity, oxidative stress response, mitochondrial dysfunction, and energy metabolism. The metabolic changes observed in the present study are thought to come as a result of PFOS inhibiting SIRT1 activity, as well as the induction of PPAR signaling pathways, because both play vital roles in the regulatory pathways of oxidative stress response and energy metabolism. Overall, the present study provides valuable insights into the embryotoxicity of PFOS in zebrafish embryos, and has enabled an integrated systems-level model of PFOS toxicity to be proposed, alongside identification of possible biomarkers of effect and exposure as potential tools for environmental biomonitoring. The findings thus contribute to our understanding of the mechanisms of PFOS toxicity, and may have utility for assessing the risks associated with PFOS exposure in aquatic organisms.

Author Contribution Statement—**Mark Annunziato**: Conceptualization; Investigation; Formal analysis; Visualization; Writing—original draft and review & editing. **Narmin Bashirova**: Investigation; Visualization. **Muhamed N. H. Eeza**: Investigation. **Ariel Lawson**: Investigation. **Francisco Fernandez-Lima**: Investigation; Visualization. **Lilian V. Tose**: Investigation, Visualization. **Jörg Matysik**: Resources; Supervision. **A. Alia**: Conceptualization; Investigation; Visualization; Writing—review & editing; Resources; Supervision. **John P. Berry**: Conceptualization; Investigation; Writing—original draft and review & editing; Supervision; Resources; Project administration; Funding acquisition.

REFERENCES

Abbott, B. D., Wolf, C. J., Das, K. P., Zehr, R. D., Schmid, J. E., Lindstrom, A. B., Strynar, M. J., & Lau, C. (2009). Developmental toxicity of perfluorooctane sulfonate (PFOS) is not dependent on expression of peroxisome proliferator activated receptor-alpha (PPARα) in the mouse. *Reproductive Toxicology*, *27*, 258–265. https://doi.org/10.1016/j.reprotox.2008.05.061

Ankley, G. T., Kuehl, D. W., Kahl, M. D., Jensen, K. M., Linnum, A., Leino, R. L., & Villeneuve, D. A. (2005). Reproductive and developmental toxicity and bioconcentration of perfluorooctanesulfonate in a partial life-cycle test with the fathead minnow (*Pimephales promelas*). *Environmental Toxicology and Chemistry*, *24*, 2316–2324. https://doi.org/10.1897/04-634R.1

Annunziato, M., Bashirova, N., Eeza, M. N. H., Lawson, A., Benetti, D., Stieglitz, J. D., Matysik, J., Alia, A., & Berry, J. P. (2023). High-resolution magic angle spinning (HRMAS) NMR identifies oxidative stress and impairment of energy metabolism by zearalenone in embryonic stages of zebrafish (*Danio rerio*), olive flounder (*Paralichthys olivaceus*) and yellowtail snapper (*Ocyurus chrysurus*). *Toxins*, *15*, 397.

Annunziato, M., Eeza, M. N. H., Bashirova, N., Lawson, A., Matysik, J., Benetti, D., Grosell, M., Stieglitz, J. D., Alia, A., & Berry, J. P. (2022). An integrated systems-level model of the toxicity of brevetoxin based on high-resolution magic-angle spinning nuclear magnetic resonance (HRMAS NMR) metabolic profiling of zebrafish embryos. *Science of the Total Environment*, *803*, 149858. https://doi.org/10.1016/j.scitotenv.2021.149858

Bashirova, N., Poppitz, D., Klüver, N., Scholz, S., Matysik, J., & Alia, A. (2023). A mechanistic understanding of the effects of polyethylene terephthalate nanoplastics in the zebrafish (*Danio rerio*) embryo. *Scientific Reports*, *13*, 1891.

Berry, J. P., Gantar, M., Gibbs, P. D., & Schmale, M. C. (2007). The zebrafish (*Danio rerio*) embryo as a model system for identification and characterization of developmental toxins from marine and freshwater microalgae. *Comparative Biochemistry and Physiology. Toxicology & pharmacology: CBP*, *145*, 61–72. https://doi.org/10.1016/j.cbpc.2006.07.011

Berry, J. P., Roy, U., Jaja-Chimedza, A., Sanchez, K., Matysik, J., & Alia, A. (2016). High-resolution magic angle spinning nuclear magnetic resonance of intact zebrafish embryos detects metabolic changes following exposure to teratogenic polymethoxyalkenes from algae. *Zebrafish*, *13*, 456–465.

Beyer, T. P., Chen, Y., Porter, R. K., Lu, D., Schmidt, R. J., Mantlo, N. B., Konrad, R. J., & Cao, G. (2008). Peroxisome proliferator-activated receptor alpha agonists regulate cholester ester transfer protein. *Lipids*, *43*, 611–618. https://doi.org/10.1007/s11745-008-3187-0

Bijland, S., Rensen, P. C. N., Pieterman, E. J., Maas, A. C. E., van der Hoorn, J. W., van Erk, M. J., Havekes, L. M., Willems van Dijk, K., Chang, S.-C., Ehresman, D. J., Butenhoff, J. L., & Princen, H. M. G. (2011). Perfluoroalkyl sulfonates cause alkyl chain length-dependent hepatic steatosis and hypolipidemia mainly by impairing lipoprotein production in APOE*3-Leiden CETP mice. *Toxicological Sciences*, *123*, 290–303. https://doi.org/10.1093/toxsci/kfr142

Bilbao, E., Raingeard, D., de Cerio, O. D., Ortiz-Zarragoitia, M., Ruiz, P., Izagirre, U., Orbea, A., Marigómez, I., Cajaraville, M. P., & Cancio, I. (2010). Effects of exposure to Prestige-like heavy fuel oil and to perfluorooctane sulfonate on conventional biomarkers and target gene transcription in the thicklip grey mullet *Chelon labrosus*. *Aquatic Toxicology*, *98*(3), 282–296. https://doi.org/10.1016/j.aquatox.2010.02.018

Borghese, M. M., Liang, C. L., Owen, J., & Fisher, M. (2022). Individual and mixture associations of perfluoroalkyl substances on liver function biomarkers in the Canadian Health Measures Survey. *Environmental Health*, *21*, 85. https://doi.org/10.1186/s12940-022-00892-6

Brand, M., Granato, M., & Nüsslein-Volhard, C. (2002). Keeping and raising zebrafish. In C. Nusslein-Volhard & R. Dahm (Eds.), *Zebrafish: A practical approach*. Oxford University Press. https://cir.nii.ac.jp/crid/1571417125721611136

Chen, X., Nie, X., Mao, J., Zhang, Y., Yin, K., Sun, P., Luo, J., Liu, Y., Jiang, S., & Sun, L. (2018). Perfluorooctane sulfonate mediates secretion of

16

Environmental Toxicology and Chemistry, 2024;00:1–19—Annunziato et al.

IL-1β through PI3K/AKT NF-κB pathway in astrocytes. *Neurotoxicology and Teratology*, 67, 65–75. https://doi.org/10.1016/j.ntt.2018.03.004

Cheng, J., Lv, S., Nie, S., Liu, J., Tong, S., Kang, N., Xiao, Y., Dong, Q., Huang, C., & Yang, D. (2016). Chronic perfluorooctane sulfonate (PFOS) exposure induces hepatic steatosis in zebrafish. *Aquatic Toxicology*, 176, 45–52. https://doi.org/10.1016/j.aquatox.2016.04.013

Christou, M., Fraser, T. W. K., Berg, V., Ropstad, E., & Kamstra, J. H. (2020). Calcium signaling as a possible mechanism behind increased locomotor response in zebrafish larvae exposed to a human relevant persistent organic pollutant mixture or PFOS. *Environmental Research*, 187, 109702. https://doi.org/10.1016/j.envres.2020.109702

Clark, J. F., Doepke, A., Filosa, J. A., Wardle, R. L., Lu, A., Meeker, T. J., & Pyne-Geithman, G. J. (2006). N-Acetylaspartate as a reservoir for glutamate. *Medical Hypotheses*, 67, 506–512. https://doi.org/10.1016/j.mehy.2006.02.047

Contreras, A. V., Rangel-Escareño, C., Torres, N., Alemán-Escondrillas, G., Ortiz, V., Noriega, L. G., Torre-Villalvazo, I., Granados, O., Velázquez-Villegas, L. A., Tobon-Cornejo, S., González-Hirschfeld, D., Recillas-Targa, F., Tejero-Barrera, E., Gonzalez, F. J., & Tovar, A. R. (2015). PPARα via HNF4α regulates the expression of genes encoding hepatic amino acid catabolizing enzymes to maintain metabolic homeostasis. *Genes & Nutrition*, 10, 1–16. https://doi.org/10.1007/s12263-014-0452-0

Cui, Y., Lv, S., Liu, J., Nie, S., Chen, J., Dong, Q., Huang, C., & Yang, D. (2017). Chronic perfluorooctanesulfonic acid exposure disrupts lipid metabolism in zebrafish. *Human & Experimental Toxicology*, 36, 207–217. https://doi.org/10.1177/0960327116646615

Deng, P., Durham, J., Liu, J., Zhang, X., Wang, C., Li, D., Gwag, T., Ma, M., & Hennig, B. (2022). Metabolomic, lipidomic, transcriptomic, and metagenomic analysis in mice exposed to PFO and fed soluble and insoluble dietary fibers. *Environmental Health Perspectives*, 130, 117003. https://doi.org/10.1289/EHP11360

Dorts, J., Kestemont, P., Marchand, P.-A., D'Hollander, W., Thézenas, M.-L., Raes, M., & Silvestre, F. (2011). Ecotoxicoproteomics in gills of the sentinel fish species, *Cottus gobio*, exposed to perfluorooctane sulfonate (PFOS). *Aquatic Toxicology*, 103, 1–8. https://doi.org/10.1016/j.aquatox.2011.01.015

Dovinova, I., Kvandová, M., Balis, P., Gresova, L., Majzunova, M., Horakova, L., Chan, J. Y., & Barancik, M. (2020). The role of Nrf2 and PPARgamma in the improvement of oxidative stress in hypertension and cardiovascular diseases. *Physiological Research*, 69, S541–s553. https://doi.org/10.33549/physiolres.934612

Du, J., Cai, J., Wang, S., & You, H. (2017). Oxidative stress and apotosis to zebrafish (*Danio rerio*) embryos exposed to perfluorooctane sulfonate (PFOS) and ZnO nanoparticles. *International Journal of Occupational Medicine and Environmental Health*, 30, 213–229. https://doi.org/10.13075/ijomeh.1896.00669

Du, Y., Shi, X., Liu, C., Yu, K., & Zhou, B. (2009). Chronic effects of waterborne PFOS exposure on growth, survival and hepatotoxicity in zebrafish: A partial life-cycle test. *Chemosphere*, 74, 723–729. https://doi.org/10.1016/j.chemosphere.2008.09.075

Duan, X., Sun, W., Sun, H., & Zhang, L. (2021). Perfluorooctane sulfonate continual exposure impairs glucose-stimulated insulin secretion via SIRT1-induced upregulation of UCP2 expression. *Environmental Pollution*, 278, 116840. https://doi.org/10.1016/j.envpol.2021.116840

Eeza, M. N. H., Bashirova, N., Zuberi, Z., Matysik, J., Berry, J. P., & Alia, A. (2022). An integregrated systems-level model of ochratoxin A toxicity in the zebrafish (*Danio rerio*) embryo based on NMR metabolic profiling. *Scientific Reports*, 12, 6341.

Foguth, R., Sepúlveda, M. S., & Cannon, J. (2020). Per- and polyfluoroalkyl substances (PFAS) neurotoxicity in sentinel and non-traditional laboratory model systems: Potential utility in predicting adverse outcomes in human health. *Toxics*, 8, 42. https://www.mdpi.com/2305-6304/8/2/42

Fraher, D., Sanigorski, A., Mellett, N. A., Meikle, P. J., Sinclair, A. J., & Gilbert, Y. (2016). Zebrafish embryobic lipidomic analysis reveals that the yolk cell is metabolically active in processing lipid. *Cell Reports*, 14, 1317–1329. https://doi.org/10.1016/j.celrep.2016.01.016

Franco, M. E., Sutherland, G. E., Fernandez-Luna, M. T., & Lavado, R. (2020). Altered expression and activity of phase I and II biotransformation enzymes in human liver cells by perfluorooctanoate (PFOA) and perfluorooctane sulfonate (PFOS). *Toxicology*, 430, 152339. https://doi.org/10.1016/j.tox.2019.152339

Gaballah, S., Swank, A., Sobus, J. R., Howey, X. M., Schmid, J., Catron, T., McCord, J., Hines, E., Strynar, M., & Tal, T. (2020). Evaluation of developmental toxicity, developmental neurotoxicity, and tissue dose in zebrafish exposed to GenX and other PFAS. *Environmental Health Perspectives*, 128, 47005. https://doi.org/10.1289/ehp5843

Gebreab, K. Y., Eeza, M. N. H., Bai, T., Zuberi, Z., Matysik, J., O'Shea, K. E., Alia, A., & Berry, J. P. (2020). Comparative toxicometabolomics of perfluorooctanoic acid (PFOA) and next-generation perfluoroalkyl substances. *Environmental Pollution*, 265, 114928. https://doi.org/10.1016/j.envpol.2020.114928

Gervois, P., Torra, I. P., Fruchart, J. C., & Staels, B. (2000). Regulation of lipid and lipoprotein metabolism by PPAR activators. *Clinical Chemistry and Laboratory Medicine*, 38, 3–11. https://doi.org/10.1515/CCLM.2000.00

Hagenaars, A., Knapen, D., Meyer, I. J., van der Ven, K., Hoff, P., & De Coen, W. (2008). Toxicity evaluation of perfluorooctane sulfonate (PFOS) in the liver of common carp (*Cyprinus carpio*). *Aquatic Toxicology*, 88, 155–163. https://doi.org/10.1016/j.aquatox.2008.04.002

Hagenaars, A., Vergauwen, L., Benoot, D., Laukens, K., & Knapen, D. (2013). Mechanistic toxicity study of perfluorooctanoic acid in zebrafish suggests mitochondrial dysfunction to play a key role in PFOA toxicity. *Chemosphere*, 91, 844–856. https://doi.org/10.1016/j.chemosphere.2013.01.056

Hagenaars, A., Vergauwen, L., De Coen, W., & Knapen, D. (2011). Structure–activity relationship assessment of four perfluorinated chemicals using a prolonged zebrafish early life stage test. *Chemosphere*, 82, 764–772. https://doi.org/10.1016/j.chemosphere.2010.10.076

Hansen, M. K., McVey, M. J., White, R. F., Legos, J. J., Brusq, J.-M., Grillot, D. A., Issandou, M., & Barone, F. C. (2010). Selective CETP inhibition and PPARalpha agonism increase HDL cholesterol and reduce LDL cholesterol in human ApoB100/human CETP transgenic mice. *Journal of Cardiovascular Pharmacology and Therapy*, 15, 196–202. https://doi.org/10.1177/1074248410362891

Higgins, A. D., Silverstein, J. T., Engles, J., Wilson, M. E., Rexroad, C. E., & Blemings, K. P. (2005). Starvation induced alterations in hepatic lysine metabolism in different families of rainbow trout (*Oncorhynchus mykiss*). *Fish Physiology and Biochemistry*, 31, 33–44. https://doi.org/10.1007/s10695-005-4587-1

Hoff, P. T., Van Campenhout, K., Van de Vijver, K., Covaci, A., Bervoets, L., Moens, L., Huyskens, G., Goemans, G., Belpaire, C., Blust, R., & De Coen, W. (2005). Perfluorooctane sulfonic acid and organohalogen pollutants in liver of three freshwater fish species in Flanders (Belgium): Relationships with biochemical and organismal effects. *Environmental Pollution*, 137, 324–333. https://doi.org/10.1016/j.envpol.2005.01.008

Hoff, P. T., Van de Vijver, K., Van Dongen, W., Esmans, E. L., Blust, R., & De Coen, W. M. (2003). Perfluorooctane sulfonic acid in bib (*Trisopterus luscus*) and plaice (*Pleuronectes platessa*) from the Western Scheldt and the Belgian North Sea: Distribution and biochemical effects. *Environmental Toxicology and Chemistry*, 22, 608–614. https://doi.org/10.1002/etc.5620220320

Honda, M., Muta, A., Akasaka, T., Inoue, Y., Shimasaki, Y., Kannan, K., Okino, N., & Oshima, Y. (2014). Identification of perfluorooctane sulfonate binding protein in the plasma of tiger pufferfish *Takifugu rubripes*. *Ecotoxicology and Environmental Safety*, 104, 409–413. https://doi.org/10.1016/j.ecoenv.2013.11.010

Huang, H., Huang, C., Wang, L., Ye, X., Bai, C., Simonich, M. T., Tanguay, R. L., & Dong, Q. (2010). Toxicity, uptake kinetics and behavior assessment in zebrafish embryos following exposure to perfluorooctanesulphonicacid (PFOS). *Aquatic Toxicology*, 98, 139–147. https://doi.org/10.1016/j.aquatox.2010.02.003

Huang, J., Wang, Q., Liu, S., Lai, H., & Tu, W. (2022). Comparative chronic toxicities of PFOS and its novel alternatives on the immune system associated with intestinal microbiota dysbiosis in adult zebrafish. *Journal of Hazardous Materials*, 425, 127950. https://doi.org/10.1016/j.jhazmat.2021.127950

Im, S. S., Kim, M. Y., Kwon, S. K., Kim, T. H., Bae, J. S., Kim, H., Kim, K. S., Oh, G. T., & Ahn, Y. H. (2011). Peroxisome proliferator-activated receptor {alpha} is responsible for the up-regulation of hepatic glucose-6-phosphatase gene expression in fasting and db/db Mice. *Journal of Biological Chemistry*, 286, 1157–1164. https://doi.org/10.1074/jbc.M110.157875

International Organization of Standardization. (2007). Water quality: Determination of the acute toxicity of waste water to zebrafish eggs (*Danio rerio*). *European Standards ISO*, 15088. https://www.iso.org/standard/37368.html

Kalous, K. S., Wynia-Smith, S. L., Olp, M. D., & Smith, B. C. (2016). Mechanism of Sirt1 NAD+-dependent protein deacetylase inhibition by

cysteine S-nitrosation. *Journal of Biological Chemistry*, *291*, 25398–25410. https://doi.org/10.1074/jbc.M116.754655

Kang, J. S., Ahn, T.-G., & Park, J.-W. (2019). Perfluorooctanoic acid (PFOA) and perfluorooctane sulfonate (PFOS) induce different modes of action in reproduction to Japanese medaka (*Oryzias latipes*). *Journal of Hazardous Materials*, *368*, 97–103. https://doi.org/10.1016/j.jhazmat.2019.01.034

Kannan, K., Tao, L., Sinclair, E., Pastva, S. D., Jude, D. J., & Giesy, J. P. (2005). Perfluorinated compounds in aquatic organisms at various trophic levels in a Great Lakes food chain. *Archives of Environmental Contamination and Toxicology*, *48*, 559–566. https://doi.org/10.1007/s00244-004-0133-x

Kaspar, J. W., Niture, S. K., & Jaiswal, A. K. (2009). Nrf2:INrf2 (Keap1) signaling in oxidative stress. *Free Radical Biology and Medicine*, *47*, 1304–1309. https://doi.org/10.1016/j.freeradbiomed.2009.07.035

Kersten, S., Mandard, S., Escher, P., Gonzalez, F. J., Tafuri, S., Desvergne, B., & Wahli, W. (2001). The peroxisome proliferator-activated receptor alpha regulates amino acid metabolism. *The FASEB Journal*, *15*, 1971–1978. https://doi.org/10.1096/fj.01-0147com

Khansari, M. R., Yousefsani, B. S., Kobarfard, F., Faizi, M., & Pourahmad, J. (2017). In vitro toxicity of perfluorooctane sulfonate on rat liver hepatocytes: Probability of distructive binding to CYP 2E1 and involvement of cellular proteolysis. *Environmental Science and Pollution Research*, *24*, 23382–23388. https://doi.org/10.1007/s11356-017-9908-2

Kim, J., Cha, Y.-N., & Surh, Y.-J. (2010). A protective role of nuclear factor-erythroid 2-related factor-2 (Nrf2) in inflammatory disorders. *Mutation Research/Fundamental and Molecular Mechanisms of Mutagenesis*, *690*, 12–23. https://doi.org/10.1016/j.mrfmmm.2009.09.007

Kosgei, V. J., Coelho, D., Guéant-Rodriguez, R.-M., & Guéant, J.-L. (2020). Sirt1-PPARS cross-talk in complex metabolic diseases and inherited disorders of the one carbon metabolism. *Cells*, *9*, 1882. https://doi.org/10.3390/cells9081882

Kowaltowski, A. J., Castilho, R. F., & Vercesi, A. E. (2001). Mitochondrial permeability transition and oxidative stress. *FEBS Letters*, *495*, 12–15. https://doi.org/10.1016/s0014-5793(01)02316-x

Krupa, P. M., Lotufo, G. R., Mylroie, E. J., May, L. K., Gust, K. A., Kimble, A. N., Jung, M. G., Boyda, J. A., Garcia-Reyero, N., & Moore, D. W. (2022). Chronic aquatic toxicity of perfluorooctane sulfonic acid (PFOS) to *Ceriodaphnia dubia*, *Chironomus dilutus*, *Danio rerio*, and *Hyalella azteca*. *Ecotoxicology and Environmental Safety*, *241*, 113838. https://doi.org/10.1016/j.ecoenv.2022.113838

Lee, H., Sung, E. J., Seo, S., Min, E. K., Lee, J.-Y., Shim, I., Kim, P., Kim, T.-Y., Lee, S., & Kim, K.-T. (2021). Integrated multi-omics analysis reveals the underlying molecular mechanism for developmental neurotoxicity of perfluorooctanesulfonic acid in zebrafish. *Environment International*, *157*, 106802. https://doi.org/10.1016/j.envint.2021.106802

Lee, Y.-M., Lee, J.-Y., Kim, M.-K., Yang, H., Lee, J.-E., Son, Y., Kho, Y., Choi, K., & Zoh, K.-D. (2020). Concentration and distribution of per- and polyfluoroalkyl substances (PFAS) in the Asan Lake area of South Korea. *Journal of Hazardous Materials*, *381*, 120909. https://doi.org/10.1016/j.jhazmat.2019.120909

Lehmler, H.-J., Xie, W., Bothun, G. D., Bummer, P. M., & Knutson, B. L. (2006). Mixing of perfluorooctane sulfonic acid (PFOS) potassium salt with dipalmitoyl phosphatidylcholine (DPPC). *Colloids and Surfaces B Biointerfaces*, *51*, 25–29. https://doi.org/10.1016/j.colsurfb.2006.05.013

Liu, C., Yu, K., Shi, X., Wang, J., Lam, P. K. S., Wu, R. S. S., & Zhou, B. (2007). Induction of oxidative stress and apoptosis by PFOS and PFOA in primary cultured hepatocytes of freshwater tilapia (*Oreochromis niloticus*). *Aquatic Toxicology*, *82*, 135–143. https://doi.org/10.1016/j.aquatox.2007.02.006

Liu, L., Shuiging, Y., Khan, R. S., Ables, G. P., Bharadwaj, K. G., Hu, Y., Huggins, L. A., Erisson, J. W., Buckett, L. K., Turnbull, A. V., Ginsberg, H. N., Blaner, W. S., Huang, L.-S., & Goldberg, I. R. (2011). DGAT1 deficiency decreases PPAR expression and does not lead to lipotoxicity in cardiac and skeletal muscle. *Journal of Lipid Research*, *52*, 732–744. https://doi.org/10.1194/jlr.M011395

Liu, L., Yu, S., Khan, R. S., Homma, S., Schulze, P. C., Blaner, W. S., Yin, Y., & Goldberg, I. J. (2012). Diacylglycerol acyl transferase 1 overexpression detoxifies cardiac lipids in PPARg transgenic mice. *Journal of Lipid Research*, *53*, 1482–1492. https://doi.org/10.1194/jlr.M024208

Mahoney, H., Cantin, J., Rybchuk, J., Xie, Y., Giesy, J. P., & Brinkmann, M. (2023). Acute exposure of zebrafish (*Danio rerio*) to the next-generation perfluoroalkyl substance, perfluoroethylcyclohexanesulfonate, shows similar effects as legacy substances. *Environmental Science & Technology*, *57*(10), 4199–4207. https://doi.org/10.1021/acs.est.2c08463

Maldonado, E. N., & Lemasters, J. J. (2014). ATP/ADP ratio, the missed connection between mitochondria and the Warburg effect. *Mitochondrion*, *19*, 78–84. https://doi.org/10.1016/j.mito.2014.09.002

Martin, J. W., Mabury, S. A., Solomon, K. R., & Muir, D. C. G. (2003). Bioconcentration and tissue distribution of perfluorinated acids in rainbow trout (*Oncorhynchus mykiss*). *Environmental Toxicology and Chemistry*, *22*, 196–204. https://doi.org/10.1002/etc.5620220126

Martínez, R., Navarro-Martín, L., Luccarelli, C., Codina, A. E., Raldúa, D., Barata, C., Tauler, R., & Piña, B. (2019). Unravelling the mechanisms of PFOS toxicity by combining morphological and transcriptomic analyses in zebrafish embryos. *Science of the Total Environment*, *674*, 462–471. https://doi.org/10.1016/j.scitotenv.2019.04.200

Moffett, J. R., Ross, B., Arun, P., Madhavarao, C. N., & Namboodiri, A. M. A. (2007). N-Acetylaspartate in the CNS: From neurodiagnostics to neurobiology. *Progress in Neurobiology*, *81*, 89–131. https://doi.org/10.1016/j.pneurobio.2006.12.003

Mylroie, J. E., Wilbanks, M. S., Kimble, A. N., To, K. T., Cox, C. S., McLeod, S. J., Gust, K. A., Moore, D. W., Perkins, E. J., & Garcia-Reyero, N. (2021). Perfluorooctanesulfonic acid-induced toxicity on zebrafish embryos in the presence or absence of the chorion. *Environmental Toxicology and Chemistry*, *40*, 780–791. https://doi.org/10.1002/etc.4899

Oakes, K. D., Sibley, P. K., Martin, J. W., Maclean, D. D., Solomon, K. R., Mabury, S. A., & Van Der Kraak, G. J. (2005). Short-term exposures of fish to perfluorooctane sulfonate: Acute effects on fatty acyl-CoA oxidase activity, oxidative stress, and circulating sex steroids. *Environmental Toxicology and Chemistry*, *24*, 1172–1181. https://doi.org/10.1897/04-419.1

Oosterveer, M. H., Grefhorst, A., van Dijk, T. H., Havinga, R., Staels, B., Kuipers, F., Groen, A. K., & Reijngoud, D. J. (2009). Fenofibrate simultaneously induces hepatic fatty acid oxidation, synthesis, and elongation in mice. *Journal of Biological Chemistry*, *284*, 34036–34044. https://doi.org/10.1074/jbc.M109.051052

Ortiz-Villanueva, E., Jaumot, J., Martínez, R., Navarro-Martín, L., Piña, B., & Tauler, R. (2018). Assessment of endocrine disruptors effects on zebrafish (*Danio rerio*) embryos by untargeted LC-HRMS metabolomic analysis. *Science of the Total Environment*, *635*, 156–166. https://doi.org/10.1016/j.scitotenv.2018.03.369

Patel, A. B., Lai, J. C., Chowdhury, G. M., Hyder, F., Rothman, D. L., Shulman, R. G., & Behar, K. L. (2014). Direct evidence for activity-dependent glucose phosphorylation in neurons with implications for the astrocyte-to-neuron lactate shuttle. *Proceedings of the National Academy of Sciences of the United States of America*, *111*, 5385–5390. https://doi.org/10.1073/pnas.1403576111

Pecquet, A. M., Maier, A., Kasper, S., Sumanas, S., & Yadav, J. (2020). Exposure to perfluorooctanoic acid (PFOA) decreases neutrophil migration response to injury in zebrafish embryos. *BMC Research Notes*, *13*, 408. https://doi.org/10.1186/s13104-020-05255-3

Peeters, A., & Baes, M. (2010). Role of PPARα in hepatic carbohydrate metabolism. *PPAR research*, *2010*, 572405. https://doi.org/10.1155/2010/572405

Popovic, M., Zaja, R., Fent, K., & Smital, T. (2014). Interaction of environmental contaminants with zebrafish organic anion transporting polypeptide, Oatp1d1 (Slco1d1). *Toxicology and Applied Pharmacology*, *280*, 149–158. https://doi.org/10.1016/j.taap.2014.07.015

Prince, N., Begum, S., Minguez-Alarcon, L., Genard-Walton, M., Huang, M., Soeteman, D. I., Wheelock, C., Litonjua, A. A., Weiss, S. T., Kelly, R. S., & Lasky-Su, J. (2023). Plasma concentrations of per- and polyfluoroalkyl substances are associated with perturbations in lipid and amino acid metabolism. *Chemosphere*, *324*, 138228. https://doi.org/10.1016/j.chemosphere.2023.138228

Ren, H., Vallanat, B., Nelson, D. M., Yeung, L. W. Y., Guruge, K. S., Lam, P. K. S., Lehman-McKeeman, L. D., & Corton, J. C. (2009). Evidence for the involvement of xenobiotic-responsive nuclear receptors in transcriptional effects upon perfluoroalkyl acid exposure in diverse species. *Reproductive Toxicology*, *27*, 266–277. https://doi.org/10.1016/j.reprotox.2008.12.011

Rhee, J., Chang, V. C., Cheng, I., Calafat, A. M., Botelho, J. C., Shearer, J. J., Sampson, J. N., Setiawan, V. W., Wilkens, L. R., Silverman, D. T., Purdue, M. P., & Hofmann, J. N. (2023). Serum concentrations of per- and polyfluoroalkyl substances and risk of renal cell carcinoma in the Multiethnic Cohort Study. *Environment International*, *180*, 108197. https://doi.org/10.1016/j.envint.2023.108197

Rosen, M. B., Das, K. P., Rooney, J., Abbott, B., Lau, C., & Corton, J. C. (2017). PPARα-independent transcriptional targets of perfluoroalkyl

acids revealed by transcript profiling. *Toxicology*, *387*, 95–107. https://doi.org/10.1016/j.tox.2017.05.013

Rosen, M. B., Schmid, J. R., Corton, J. C., Zehr, R. D., Das, K. P., Abbott, B. D., & Lau, C. (2010). Gene expression profiling in wild-type and PPARα-null mice exposed to perfluorooctane sulfonate reveals PPARα-independent effects. *PPAR research*, *2010*, 794739. https://doi.org/10.1155/2010/794739

Roy, U., Conklin, L., Schiller, J., Matysik, J., Berry, J. P., & Alia, A. (2017). Metabolic profiling of of zebrafish (*Danio rerio*) embryos by NMR spectroscopy reveals multifaceted toxicity of β-methylamino-L-alanine (BMAA). *Scientific Reports*, *7*, 17305.

Sandhofer, A., Kaser, S., Ritsch, A., Laimer, M., Engl, J., Paulweber, B., Patsch, J. R., & Ebenbichler, C. F. (2006). Cholesteryl ester transfer protein in metabolic syndrome. *Obesity*, *14*, 812. https://doi.org/10.1038/oby.2006.94-818

Sant, K. E., Sinno, P. P., Jacobs, H. M., & Timme-Laragy, A. R. (2018). Nrf2a modulates the embryonic antioxidant response to perfluorooctanesulfonic acid (PFOS) in the zebrafish, *Danio rerio*. *Aquatic Toxicology*, *198*, 92–102. https://doi.org/10.1016/j.aquatox.2018.02.010

Schaffer, S. W., Azuma, J., & Mozaffari, M. (2009). Role of antioxidant activity of taurine in diabetes. *Canadian Journal of Physiology and Pharmacology*, *87*, 91–99. https://doi.org/10.1139/y08-110

Schuler, M.-H., Di Bartolomeo, F., Mårtensson, C. U., Daum, G., & Becker, T. (2016). Phosphatidylcholine affects inner membrane protein translocases of mitochondria. *The Journal of Biological Chemistry*, *291*, 18718–18729. https://doi.org/10.1074/jbc.M116.722694

Seyoum, A., Pradhan, A., Jass, J., & Olsson, P.-E. (2020). Perfluorinated alkylsubstances impede growth, reproduction, lipid metabolism and lifespan in *Daphnia magna*. *Science of the Total Environment*, *737*, 139682. https://doi.org/10.1016/j.scitotenv.2020.139682

Shi, X., Du, Y., Lam, P. K. S., Wu, R. S. S., & Zhou, B. (2008). Developmental toxicity and alteration of gene expression in zebrafish embryos exposed to PFOS. *Toxicology and Applied Pharmacology*, *230*, 23–32. https://doi.org/10.1016/j.taap.2008.01.043

Shi, X., Liu, C., Wu, G., & Zhou, B. (2009). Waterborne exposure to PFOS causes disruption of the hypothalamus–pituitary–thyroid axis in zebrafish larvae. *Chemosphere*, *77*, 1010–1018. https://doi.org/10.1016/j.chemosphere.2009.07.074

Shi, X., & Zhou, B. (2010). The role of Nrf2 and MAPK pathways in PFOS-induced oxidative stress in zebrafish embryos. *Toxicological Sciences*, *115*, 391–400. https://doi.org/10.1093/toxsci/kfq066

Sinclair, E., Mayack, D. T., Roblee, K., Yamashita, N., & Kannan, K. (2006). Occurrence of perfluoroalkyl surfactants in water, fish, and birds from New York state. *Archives of Environmental Contamination and Toxicology*, *50*, 398–410. https://doi.org/10.1007/s00244-005-1188-z

Sun, Q., Jia, N., Yang, J., & Chen, G. (2018). Nrf2 signaling pathway mediates the antioxidative effects of taurine against corticosterone-induced cell death in HUMAN SK-N-SH cells. *Neurochemical Research*, *43*, 276–286. https://doi.org/10.1007/s11064-017-2419-1

Takacs, M. L., & Abbott, B. D. (2006). Activation of mouse and human peroxisome proliferator–activated receptors (α, β/δ, γ) by perfluorooctanoic acid and perfluorooctane sulfonate. *Toxicological Sciences*, *95*, 108–117. https://doi.org/10.1093/toxsci/kfl135

Tobón-Cornejo, S., Vargas-Castillo, A., Leyva-Martínez, A., Ortíz, V., Noriega, L. G., Velázquez-Villegas, L. A., Aleman, G., Furosawa-Carballeda, J., Torres, N., & Tovar, A. R. (2021). PPARα/RXRα downregulates amino acid catabolism in the liver via interaction with HNF4α promoting its proteasomal degradation. *Metabolism: Clinical and Experimental*, *116*, 154705. https://doi.org/10.1016/j.metabol.2021.154705

Valsecchi, S., Babut, M., Mazzoni, M., Pascariello, S., Ferrario, C., De Felice, B., Bettinetti, R., Veyrand, B., Marchand, P., & Polesello, S. (2021). Per- and polyfluoroalkyl substances (PFAS) in fish from European Lakes: Current contamination status, sources, and perspectives for monitoring. *Environmental Toxicology and Chemistry*, *40*, 658–676. https://doi.org/10.1002/etc.4815

van Amerongen, Y. F., Roy, U., Spaink, H. P., de Groot, H. J. M., Huster, D., Schiller, J., & Alia, A. (2014). Zebrafish brain lipid characterization and quantification by 1H nuclear magnetic resonance spectroscopy and MALDI-TOF mass spectrometry. *Zebrafish*, *11*, 240–247. https://doi.org/10.1089/zeb.2013.0955

Verrier, E., Wang, L., Wadham, C., Albanese, N., Hahn, C., Gamble, J. R., Krishna, V., Chatterjee, K., Vadas, M. A., & Xia, P. (2004). PPARgamma agonists ameliorate endothelial cell activation via inhibition of diacylglycerol-protein kinase C signaling pathway: Role of diacylglycerol kinase. *Circulation Research*, *94*, 1515–1522. https://doi.org/10.1161/01.RES.0000130527.92537.06

Vogs, C., Johanson, G., Naslund, M., Wulff, S., Sjodin, M., Hellstrandh, M., Lindberg, J., & Wincent, E. (2019). Toxicokinetics of perfluorinated alkyl acids influences their toxic potency in the zebrafish embryo (*Danio rerio*). *Environmental Science and Technology*, *53*, 3898–3907.

Wan, H. T., Cheung, L. Y., Chan, T. F., Li, M., Lai, K. P., & Wong, C. K. C. (2021). Characterization of PFOS toxicity on in-vivo and ex-vivo mouse pancreatic islets. *Environmental Pollution*, *289*, 117857. https://doi.org/10.1016/j.envpol.2021.117857

Wang, L., Wang, Y., Liang, Y., Li, J., Liu, Y., Zhang, J., Zhang, A., Fu, J., & Jiang, G. (2014). PFOS induced lipid metabolism disturbances in BALB/c mice through inhibition of low density lipoproteins excretion. *Scientific Reports*, *4*, 4582. https://doi.org/10.1038/srep04582

Wang, T., Wang, Y., Liao, C., Cai, Y., & Jiang, G. (2009). Perspectives on the inclusion of perfluorooctane sulfonate into the Stockholm Convention on persistent organic pollutants. *Environmental Science & Technology*, *43*, 5171–5175. https://doi.org/10.1021/es900464a

Warner, R. M., Sweeney, L. M., Hayhurst, B. A., & Mayo, M. L. (2022). Toxicokinetic modeling of per- and polyfluoroalkyl substance concentrations within developing zebrafish (*Danio rerio*) populations. *Environmental Science & Technology*, *56*, 13189–13199. https://doi.org/10.1021/acs.est.2c02942

Weiss-Errico, M. J., Berry, J. P., & O'Shea, K. E. (2017). β-Cyclodextrin attenuates perfluorooctanoic acid toxicity in the zebrafish embryo model. *Toxics*, *5*, 31. https://www.mdpi.com/2305-6304/5/4/31

Wilson, D. F. (2017). Oxidative phosphorylation: Unique regulatory mechanism and role in metabolic homeostasis. *Journal of Applied Physiology*, *122*, 611–619. https://doi.org/10.1152/japplphysiol.00715.2016

Wu, L., Dang, Y., Liang, L.-X., Gong, Y.-C., Zeeshan, M., Qian, Z., Geiger, S. D., Vaughn, M. G., Zhou, Y., Li, Q.-Q., Chu, C., Tan, Y.-W., Lin, L.-Z., Liu, R.-Q., Hu, L.-W., Yang, B.-Y., Zeng, X.-W., Yu, Y., & Dong, G.-H. (2022). Perfluorooctane sulfonates induces neurobehavioral changes and increases dopamine neurotransmitter levels in zebrafish larvae. *Chemosphere (Oxford)*, *297*, 134234. https://doi.org/10.1016/j.chemosphere.2022.134234

Wu, P., Peters, J. M., & Harris, R. A. (2001). Adaptive increase in pyruvate dehydrogenase kinase 4 during starvation is mediated by peroxisome proliferator-activated receptor α. *Biochemical and Biophysical Research Communications*, *287*, 391–396. https://doi.org/10.1006/bbrc.2001.5608

Xie, W., Ludewig, G., Wang, K., & Lehmler, H.-J. (2010). Model and cell membrane partitioning of perfluorooctanesulfonate is independent of the lipid chain length. *Colloids and Surfaces B Biointerfaces*, *76*, 128. https://doi.org/10.1016/j.colsurfb.2009.10.025

Xu, H., Zhang, H., Zhang, J., Huang, Q., Shen, Z., & Wu, R. (2016). Evaluation of neuron-glia integrity by in vivo proton magnetic resonance spectroscopy: Implications for psychiatric disorders. *Neuroscience & Biobehavioral Reviews*, *71*, 563–577. https://doi.org/10.1016/j.neubiorev.2016.09.027

Xu, J.-J., Cui, J., Lin, Q., Chen, X.-Y., Zhang, J., Gao, E.-H., Wei, B., & Zhao, W. (2021). Protection of the enhanced Nrf2 deacetylation and its downstream transcriptional activity by SIRT1 in myocardial ischemia/reperfusion injury. *International Journal of Cardiology*, *342*, 82–93. https://doi.org/10.1016/j.ijcard.2021.08.007

Xu, X., Song, Z., Mao, B., & Xu, G. (2022). Apolipoprotein A1-related proteins and reverse cholesterol transport in antiatherosclerosis therapy: Recent progress and future perspectives. *Cardiovascular Therapeutics*, *2022*, 4610834. https://doi.org/10.1155/2022/4610834

Yang, C.-H., Glover, K. P., & Han, X. (2010). Characterization of cellular uptake of perfluorooctanoate via organic anion-transporting polypeptide 1A2, organic anion Transporter 4, and urate Transporter 1 for their potential roles in mediating human renal reabsorption of perfluorocarboxylates. *Toxicological Sciences*, *117*, 294–302. https://doi.org/10.1093/toxsci/kfq219

Yang, W., Ling, X., He, S., Cui, H., Yang, Z., An, H., Wang, L., Zou, P., Chen, Q., Liu, J., Ao, L., & Cao, J. (2023). PPARα/ACOX1 as a novel target for hepatic lipid metabolism disorders induced by per- and polyfluoroalkyl substances: An integrated approach. *Environment International*, *178*, 108138. https://doi.org/10.1016/j.envint.2023.108138

Yoo, H. C., Yu, Y. C., Sung, Y., & Han, J. M. (2020). Glutamine reliance in cell metabolism. *Experimental & Molecular Medicine*, *52*, 1496–1516. https://doi.org/10.1038/s12276-020-00504-8

Zhang, C., McElroy, A. C., Liberatore, H. K., Alexander, N. L. M., & Knappe, D. R. U. (2021). Stability of per- and polyfluoroalkyl substances in solvents relevant to environmental and toxicological analysis. *Environmental Science and Technology*, *56*, 6103–6112. https://doi.org/10.1021/acs.est.1c03979

Zhang, Y.-Y., Tang, L.-L., Zheng, B., Ge, R.-S., & Zhu, D.-Y. (2016). Protein profiles of cardiomyocyte differentiation in murine embryonic stem cells exposed to perfluorooctane sulfonate. *Journal of Applied Toxicology*, *36*, 726–740. https://doi.org/10.1002/jat.3207

Zhao, G., Wang, J., Wang, X., Chen, S., Zhao, Y., Gu, F., Xu, A., & Wu, L. (2011). Mutagenicity of PFOA in mammalian cells: Role of mitochondria-dependent reactive oxygen species. *Environmental Science & Technology*, *45*, 1638–1644. https://doi.org/10.1021/es1026129

Zheng, F., Sheng, N., Zhang, H., Yan, S., Zhang, J., & Wang, J. (2017). Perfluorooctanoic acid exposure disturbs glucose metabolism in mouse liver. *Toxicology and Applied Pharmacology*, *335*, 41–48. https://doi.org/10.1016/j.taap.2017.09.019

Zuberi, Z., Eeza, M. N. H., Matysik, J., Berry, J. P., & Alia, A. (2019). NMR-based metabolic profiles of intact zebrafish embryos exposed to aflatoxin A1 recapitulates hepatoxicity and supports possible neurotoxicity. *Toxins*, *11*, 258.